Accepted Manuscript

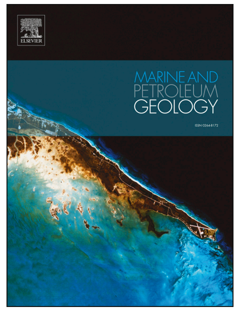

Rift-margin extensional forced folds and salt tectonics in the eastern Basque-Cantabrian rift basin (western Pyrenees)

A. Bodego, E. Iriarte, M.A. López-Horgue, I. Álvarez

PII: S0264-8172(18)30051-5

DOI: 10.1016/j.marpetgeo.2018.02.007

Reference: JMPG 3235

To appear in: *Marine and Petroleum Geology*

Received Date: 28 November 2017

Revised Date: 2 February 2018

Accepted Date: 6 February 2018

Please cite this article as: Bodego, A., Iriarte, E., López-Horgue, M.A., Álvarez, I., Rift-margin extensional forced folds and salt tectonics in the eastern Basque-Cantabrian rift basin (western Pyrenees), *Marine and Petroleum Geology* (2018), doi: 10.1016/j.marpetgeo.2018.02.007.

Rift-margin extensional forced folds and salt tectonics in the eastern Basque-Cantabrian rift basin (western Pyrenees)

Rift-margin extensional forced folds

Authors: Bodego, A.[1], Iriarte, E.[2], López-Horgue, M. A. [1], Álvarez, I.[3]

[1] Department of Stratigraphy and Palaeontology, Faculty of Science and Technology, University of the Basque Country UPV/EHU, 48080 Bilbao, Spain. E-mail address:arantxa.bodego@ehu.eus; mikel.lopez-horgue@ehu.eus

[2] Department of Historical Sciences and Geography, Laboratory of Human Evolution, University of Burgos, 09001 Burgos, Spain. E-mail address: eiriarte@ubu.es

[3] Department of Graphical Expression and Engineering Projects, Engineering School of Bilbao, University of the Basque Country UPV/EHU, 48013 Bilbao, Spain. E-mail address: irantzu.alvarez@ehu.eus

Corresponding author:

Arantxa Bodego

Department of Stratigraphy and Palaeontology

Faculty of Science and Technology

University of the Basque Country (UPV/EHU)

Sarriena auzoa z/g, 48940 Leioa, Bizkaia, Spain

Abstract:

In this paper we present and discuss Cretaceous extensional folds of the eastern Basque-Cantabrian Basin (Northern Spain). Geometry and kinematics of folds is constrained by means of structural and sedimentological fieldwork integrated with geological mapping, revealing an intimate link between coeval folding, extensional faulting, and salt mobilization. In detail, the Mesozoic succession of the northwestern and southern borders of the Palaeozoic Bortziriak-Cinco Villas massif (eastern margin of the BCB) host late Albian–early Cenomanian syn-rift forced folds. The studied forced fold axes trend parallel and are located above main and inferred Cretaceous syn-sedimentary basement faults. Structural data indicate that these folds formed during the late Albian − early Cenomanian interval. The presence of Upper Triassic clay and evaporite outcrops along and/or close to the axes of folds and their stratigraphic relationship with Upper Cretaceous strata indicate their halokinetic origin and extrusion during folding. The trigger of salt tectonics is attributed to a basement extensional pulse during the Bay of Biscay – Pyrenean rifting. Related high subsidence-rates allowed salt to flow towards faults, forming salt walls and causing the inflation and folding of the overburden.

Keywords: forced folds; rift margin; salt tectonics; extension; Cretaceous; Basque-Cantabrian basin

(A) INTRODUCTION

It has been widely reported that the presence of an intra-stratal decollement layer controls the mode of extension in rift basins (e.g. Morley and Guerin, 1996; Stewart et al., 1997; Rowan et al., 2004; Tvedt et al., 2013; Martin-Martin et al., 2016). This viscous layer, which may be either overpressured shale or salt, influences the degree of coupling between the sub- and supra-decollement deformation (Morley and Guerin, 1996; Rowan et al., 2004). In rift settings with ongoing basement extension, the presence of an efficient decollement layer may inhibit the upward propagation of basement-involved faults into the supra-decollement sedimentary cover (e.g. Stearns, 1978; Brown, 1980; Laubscher, 1982; Withjack et al., 1990). Therefore, coeval thick-skinned (basement-involved) and thin-skinned tectonics (faults that are wholly restricted to supra-decollement strata) may occur in these extensional settings, as the thin-skinned faulting directly balances basement-involved extension (e.g. Stewart et al., 1997; Pascoe et al., 1999; Withjack and Callway, 2000; Lewis et al., 2013; Wilson et al., 2013).

If the decollement level is formed by salt, the activity of sub- and supra-decollement faults can trigger halokinesis. In that context, the development of folds, faults and salt structures in the supra-salt sedimentary cover results from the coeval sub-basement extension and lateral flow of the viscous salt layer (Withjack et al., 1990; Sharp et al., 2000; Richardson et al., 2005). Extensional forced folds typically form in such a context (Laubscher, 1982). This kind of fold is defined by a monocline in the supra-salt cover, dipping as the underlying basement fault. The monocline divides an anticline and a syncline, which develop above the footwall and hanging-wall cutoff points of the top of the pre-salt, respectively. Despite many examples of forced folds can be found in the literature, most of them are based on seismic line interpretation (e.g. Maurin and Niviere, 2000; Richardson et al., 2005) or analogue and numerical modelling (e.g. Withjack et al., 1990), but limited information is available on outcrop analogue (Bodego and Agirrezabala, 2013; Tavani and Granado, 2015).

In this work we present outcrop data of extensional forced folds from the northeastern portion of the Basque-Cantabrian Basin. There, the occurrence of a pre-rift Triassic salt layer imposed decoupling between the supra- and sub-salt rocks during Cretaceous rifting. The described structures are slightly overprinted by contractional and/or inversion tectonics but preserve the original stratigraphic and structural relationship. Thus, this allows us to depict the age of the tectonic activity and salt-structure formation and its impact on the ongoing marine sedimentation. The integration of the data within the context of the Cretaceous Bay of Biscay-Pyrenean rifting, allows us to illustrate the mode of extension of the supra-decollement cover decoupled from the sub-decollement basement under an active extensional phase and its stratigraphic and sedimentary impact. It permits also to advance in the discussion about the possible compressional tectonic event in the BCB and Pyrenean realm during the latest Albian-Early Cenomanian rifting, since here is presented an alternative way to explain the creation of apparently compressional folds that support that assumption.

(A) GEOLOGICAL OUTLINE

(B) Regional tectonics and halokinesis during the Cretaceous rifting of the Basque-Cantabrian basin

The studied area is located at the eastern portion of the Basque-Cantabrian basin (BCB), being part of the Cretaceous Bay of Biscay-Pyrenean rift system (Fig. 1A), presently incorporated into the Pyrenean Orogenic System. The studied forced folds crop out around the Bortziriak-Cinco Villas Palaeozoic Massif (Bortziriak massif hereafter) (Fig. 1B). During the Mesozoic rifting, this massif represented the northeastern margin of the E-W elongated BCB and was located on the NNE-SSW striking transfer zone between this basin and the Mauleon basin to the east, in the segmented Pyrenean−Basque-Cantabrian rift system (Tugend *et al*. 2014). BCB development is intimately linked to the evolution of the southern North Atlantic, which resulted in the opening of the Bay of Biscay and other Pyrenean rift basins during the Mesozoic, under extensional to transtensional tectonics (i.e. Choukroune and Mattauer, 1978; Montadert et al., 1979; García-Mondéjar *et al*., 1996; Roca et al., 2011; Tugend *et al*., 2014). The basin underwent successive rifting events, and for the Aptian-early Cenomanian interval, thick rift successions, up to 14 km, deposited in the area (Camara, 1997). Late Cretaceous-Cenozoic convergence between the Iberian and the European Plates resulted in basin inversion (Boillot and Malod, 1988; Tugend et al., 2014).

In the BCB, syn-sedimentary structures linked to salt mobilization due to extensional tectonics have been widely described. Some of these structures were described as halokinetic features from the Upper Jurassic–Lower Cretaceous of the western BCB (e.g. Tavani et al., 2013; Tavani and Granado 2015), lower Aptian of the central BCB (e.g. García-Mondéjar, 1979, 1982; García-Mondéjar and García-Pascual, 1982; Badillo, 1982; Agirrezabala and García-Mondéjar, 1989), and from the Albian of the western, central and eastern BCB (García-Mondéjar and Robador, 1986-1987; García-Mondéjar et al., 1996; López-Horgue et al., 2010; Bodego and Agirrezabala, 2013; Poprawski et al., 2014, 2016). All these authors conclude that the formation of salt structures was intimately linked to the activity of basement faults. Moreover, some of the most important diapirs are located at the intersection between major Hercynian basement faults reactivated during the Cretaceous rifting episode (García-Mondéjar et al., 1996).

Similarly, other adjacent Pyrenean and Bay of Biscay basins record similar halokinetic episodes. Several diapiric structures have been described from the Aptian-Lower Cenomanian of the Pyrenean rift basins (e.g. Canérot and Delavaux, 1986; Canérot, 1989; Canérot and Lenoble, 1993; Canérot et al., 2005; Lagabrielle and Bodinier, 2008; Lagabrielle et al., 2010; Jammes et al., 2010) and the Parentis basin (e.g. Jammes et al., 2010; Ferrer et al., 2012, 2014). Most of these salt structures were also related to basement faults that had an important role in the extension of these rift basins.

(B) The Bortziriak massif: stratigraphy

The studied outcrops are located in the northeastern and southern margin of the Bortziriak massif (NW margin and S margin, hereafter) (Figs. 2, 3 and 4). The study area includes a Palaeozoic to Cretaceous stratigraphic succession, which records multiple deformation events (Fig. 2) (Lamare, 1936; Rat, 1959; Campos, 1979; Bodego et al., 2015). The Variscan basement is composed of Palaeozoic metasediments (Heddebaut, 1973, 1975; Requadt, 1974; Campos, 1979) and they are overlain by Lower Triassic red beds (Buntsandstein facies) in angular unconformity. For the sake of the simplicity, Palaeozoic to Lower Triassic rocks will be named (sub-decollement) basement henceforth. Upper Triassic red clays and evaporites (Keuper facies) overlie this basement. Keuper rocks constitute the main decollement layer in the BCB both for thin-skinned extensional (Fort et al., 2004; Serrano and Martinez del Olmo, 2004, Bodego and Agirrezabala, 2013; Tavani et al., 2013, Tavani and Granado, 2015) and contractional (Capote et al., 2002) structures. Thus, present day outcrops of Upper Triassic rocks in the BCB show great thickness variations due to post-depositional salt tectonics and diapirism.

The supra-decollement Jurassic to lower Cenomanian succession consists of a mixed carbonate and siliciclastic sequence, deposited during different rifting pulses. This succession comprises pre- and syn-folding strata (Fig. 2). Jurassic marls and limestones overlie Triassic red clays and evaporites, which in turn are overlain by Lower Cretaceous (Neocomian) limestones and marls ("Serpulid limestones", Soler y José, 1972). The middle Cretaceous sequence (Bodego et al., 2015) starts with lower Aptian Errenaga Fm. consisting of shallow marine carbonate platform and trough marls and limestones whereas the upper Aptian to lower Albian Buruntza limestone Fm. is compound of shallow-marine carbonates. The overlying upper Albian Azkorte sandstone Fm. comprises estuarine sandstones, which in turn are overlain by upper Albian to lower Cenomanian siliclastic shelf mudstones of the Oztaran Fm. and prodelta mudstones of the Oriamendi Fm. The coeval Oiartzun Fm. comprises limestones, sandstones and conglomerates of a braid-plain delta environments in more coastal areas.

Syn-folding regional strata in the NW margin correspond to the Lasarte megabreccia Fm., and are composed of deep-water mudstone megabreccia with olistoliths. In the S margin, shallow-marine limestone breccias with sandy matrix of the Kostartzu breccia Fm. compound the syn-folding unit. The syn-folding strata overlie the latest Albian – earliest Cenomanian U1 unconformity surface, characterized by disconformity, angular unconformity and progressive angular unconformity features. The post-folding middle Cenomanian to Campanian Upper Cretaceous Calcareous Flysch, comprising alternating hemipelagic marls and limestones (Mathey, 1987), unconformably overlie the pre- and syn-folding strata, above the U2 surface (Iriarte and Caron, 2003). This discontinuity is characterized by disconformity and angular unconformity surfaces, as well as pervasive boring, iron oxide crusts and hardground features.

(B) Cretaceous syn-sedimentary basement faults

Aptian-Albian syn-rift deposits of the BCB are controlled by major NW-SE trending and minor E-W-, NE-SW-, and N-S-trending basement faults, that compartmentalized the basin producing a complex uplifted and subsident block pattern (García-Mondéjar et al., 1996). In the studied area, main NW-SE trending structures (e.g. Ereñozu fault; Fig. 3) and E-W trending faults (Errekalde – Aritxulegi faults in the NW area, Fig. 3; and Leitza fault in the southern area, Fig. 4) controlled the compartmentation of the basin margin.

(C) The Errekalde fault (Fig. 3)

The E-W trending Errekalde fault (Lamare, 1936) is one of the main faults of the NW margin (Fig. 3A,B, Fig. 5A), and coincides with the axis of the Errekalde anticlinal fold where small Upper Triassic Keuper outcrops appear (Fig. 5B). The trend of this fault coincides with the trend of the Aritxulegi fault, which can be traced along 30 km to the west until the Bera basin. The Aptian-early Cenomanian syn-sedimentary activity of the Errekalde fault has been previously described (Bodego et al., 2008; Bodego and Agirrezabala, 2013), since this fault delimited a highly subsiding southern block in the western part (Lasarte sub-basin, Bodego and Agirrezabala, 2013). To the east, the Errekalde and Aritxulegi faults differentiated a northern subsident block during the late Albian-early Cenomanian (i.e. sedimentation of thick Oiartzun Fm. deposits around the Oiartzun anticline), from a southern uplifted block, where only isolated limestone-patches of the Oiartzun Fm. were deposited on top of the uplifted basement (Fig. 3A).

The Aptian-Lower Cenomanian activity of the fault is evidenced by the stratigraphy of its blocks. The northern footwall shows thinner pre-folding strata (only about 200 m of Aptian-Albian deposits) in comparison with the southern hanging-wall (up to 1000 m of Aptian-Albian deposits) (Fig. 5C). Moreover, the hanging-wall records thick syn-folding strata (427 m, Lasarte megabreccia Fm.), whereas in the footwall, only a small outcrop (30-50 m thick) of syn-folding strata is visible, and is confined to a small canyon geometry (Fig. 5A,B).

(C) The Txoritokieta fault (Fig. 3)

In the northwest margin, NW-SE trending faults appear to the north of the Errekalde and Aritxulegi faults (Fig. 3A,B). These faults approximately coincide with the axis of the Txoritokieta anticline (Fig. 6A,B). The southeastern end of the Txoritokieta fault trace is overlain by Upper Cretaceous rocks. Keuper clays and evaporites crop out along its trace. Lower Cretaceous stratigraphic thickness differences across the faults suggest its Cretaceous (Albian-Lower Cenomanian) normal play. Westward, the parallel Oiartzun fault shows similar stratigraphic characters.

The upper Albian–lower Cenomanian stratigraphy of the hanging-wall and footwall differs considerably (Fig. 6C). The SW footwall is only visible in the northwestern area of the fold, and shows 170 m of Oiartzun Fm. limestones disconformably overlying Jurassic strata. The NE hanging-wall shows a more complex stratigraphy. Where visible (only towards the NW end of the fold axis), the Oiartzun Fm. overlies disconformably Jurassic strata. However, most of the base of the Oiartzun Fm. shows a tectonic (faulted) contact with Keuper rocks and locally, with Neocomian and early Aptian strata. In this NE block, the Oiartzun Fm. shows a thicker succession of up to 830 m. The succession starts with shallow marine fine-grained sandstones, which are overlain by shallow marine limestones and lateral changes to braid-plain delta sandstones. Deltaic conglomerates and sandstones disconformably overlie the limestones and sandstones (Fig. 6).

(C) The Bertiz fault (Fig. 4)

The Bertiz fault belongs to a system of NNW-SSE-striking extensional faults exposed at the southern margin of the Bortziriak massif (Fig. 4). Most of them were active during the deposition of mid-Cretaceous layers, and in the case of the Bertiz fault for the upper Albian, giving rise to a small tectonic graben (Oieregi through, Fig. 4B) and escarpment breccias along its trace (Iriarte, 2004; Bodego et al., 2015). All these faults are E-dipping and abut southward against the E-W trending Leitza fault. This is a deeply rooted main fault, evidenced by the presence of a wide band (up to 3 km) of HT/LT Cretaceous metamorphic rocks (*Marble Nappe*; Lamare, 1936; Ravier, 1959; Albarede and Michard-Vitrac, 1978) and granulite, migmatite and lherzolite bodies of crustal and mantle origin (Mendia and Gil-Ibarguchi, 1991; DeFelipe et al., 2017).

The (pre-folding) stratigraphic thickness of the footwall, NE limb of the anticline (Fig. 7A,B), is reduced (100 m, Buruntza Fm.), compared to the adjacent stratigraphy of the block to the SW of the Oronoz fault (342 m of Buruntza and Azkorte Fms. strata), and particularly, to the SW block of the Bertiz fault (570 m of Buruntza and Azkorte Fms. strata)(Fig. 7C). The Bertiz and Oronoz faults acted as normal faults during the Aptian-Albian, therefore allowing deposition of thicker successions towards the SW (Iriarte, 2004).

(A) FORCED FOLDS

NW-SE and E-W oriented folds, deforming supra-decollement Jurassic to mid-Cretaceous strata and related to previously mentioned basement faults, have been mapped in the study area (Fig. 3A,4A). In some of them, accurately characterized for this work, original stratigraphic and structural features are observed, depicting the age and mechanism of their formation and its impact on the ongoing marine sedimentation. In the NW margin of the Bortziriak massif, folds strike defines two patterns (Fig. 3B): E-W (Errekalde antilcline) and NW-SE (Txoritokieta and Oiartzun anticlines, along with the Arizmendi syncline). In the southern margin of the Bortziriak massif the same pattern is repeated: NW-SE − trending folds developed along NW-SE trending faults (e.g. the Mugaire anticline) which are located to the north and obliquely to the E-W trending Leitza fault (Fig. 4B).

The anticlines are cored by faults and the Keuper evaporites crop out along these faults (Fig. 5A,6A,7A), indicating their genesis as salt cored faulted anticlines. Moreover, precise dating of post-folding strata of two anticlines indicates that Keuper rocks were extruded to the sea floor by the latest Albian-early Cenomanian. In the case of the Oiartzun anticline, the contact between post-folding and syn- or pre-folding strata is tectonic, and thus, no stratigraphic dating of the folding event was possible.

In the following sub-sections, we describe three key examples of faulted anticlines in order to constrain the characteristics and controlling processes of these types of folds: the Errekalde and Txoritokieta forced folds in the NW margin, and the Mugaire forced fold in the S margin.

(B) The E-W Errekalde faulted anticline

This is a tight anticline (“le brachyanticlinal de Recalde-Hernani”; Lamare, 1936) that strikes N114ºE and shows a northern vergence. Its hinge zone is cored by the Errekalde fault that shows Keuper rocks along its trace (Fig. 5A). Its northern limb is overturned and dips 75º to the south (Fig. 5B). The trace of the anticline disappears to the east beneath the post-folding Upper Cretaceous rocks and Quaternary alluvial deposits. Westward, the anticline is eroded by an angular to progressive unconformity (U1) depicted by syn-folding sedimentation of the Lasarte megabreccia Fm. (Bodego et al., 2008)(Fig. 5B). These deposits, composed of polimictic megabreccia of latest Albian-earliest Cenomanian age, are attributed to the erosion of a growth fold (Bodego et al., 2008). In the northern limb, U2 is a low-angle angular unconformity on top of upper Albian pre-folding rocks. In the southern limb this contact is not visible due to actual erosion.

(C) Structural restoration of the Errekalde faulted anticline

The structural data has been restored considering a horizontal datum of the base of the post-folding Upper Cretaceous strata (Fig. 5D). That restoration shows that during the deposition of the first post-folding strata (latest early Cenomanian age, *Rotalipora globotruncanoides* planktic foraminifera biozone) (Bodego et al., 2008), the pre-folding strata of the northern limb of the anticline dip 15º towards the NE (15/046). On the other hand, the pre-folding strata of the southern limb were inverted and dipping 35º towards the NNE (35/015). Therefore, this limb suffered a rotation of 145º during the latest Albian – earliest Cenomanian. The orientation of the axial plane is 25/024 and the limbs show an angle of 20º between them, with an axis dipping 11º towards the east. Thus, the restored latest Albian–earliest Cenomanian anticline structure shows recumbent fold geometry (assuming no alpine contractional refolding). The outcrops of Keuper material along the hinge of this structure that terminate against the U1 surface, indicate that the anticlinal was faulted and Keuper material extruded through this fault at least by the time of U1 formation and Lasarte Megabreccia deposition.

(B) The NW-SE Txoritokieta faulted anticline

This is a NW-SE striking anticline cored by a NW-SE striking and kilometer long high-angle reverse-fault, with large volumes of Keuper cropping out along and around the trace of the fault (Fig. 6A). In the NW area, the hinge area presents a dense network of decametric to hectometric faults, that put together narrow blocks with distinct stratigraphy. In the SW limb, strata between the U2 and U1 unconformities and below the U1 unconformity dip 15º toward the SW. In the NE limb the U1 unconformity is not occurring, and strata below the U2 unconformity dip 37º to the NE. Upper Cretaceous (lower Santonian to upper Campanian) post-folding strata on top of the U2 unconformity dip toward the SW on both limbs, with similar dip values but different unconformity angles, evidencing a pre-U2 folding (Figs. 6A,B). Similarly, the post-folding strata overlie and fossilize the described faults and the hinge of the anticline. Towards the hinge of the anticline the base of the Upper Cretaceous post-folding marls are in contact with older deposits (limestones) of the Oiartzun Fm. by an irregular erosive surface (Fig. 8A,B), and also overlie unconformably Keuper rocks (Fig. 8C).

Both limbs present subvertical sediment filled meter to decametre scale planar fissures and joints in the limestones of the Oiartzun Fm. In the SW limb these fissures appear on top of the limestone lithosome (U2 surface) and are filled (postdated) with post-folding Upper Cretaceous marls (Fig. 8D). The NE limb also shows fissures filled with post-folding marls. Nevertheless, limestones of the Oiartzun Fm. (not in the U2 surface) show also slightly older planar fissures filled with calcarenites and sandstones from the Oiartzun Fm. (neptunian dykes, Fig. 8E). Besides, U2 surface shows pervasive boring, iron oxide crusts and hardground features (Fig. 8F).

(C) Restoration of the Txoritokieta faulted anticline

The structural data has been restored considering the datum of the post-folding Upper Cretaceous flysch strata (Fig. 6D). Though diachronic, these strata are interpreted to be deposited horizontally on top of the fold.

The structural restoration to the base of the post-folding strata (U2) shows the presence of a previous faulted open anticline. The orientation of the NE limb is 79/048 and of the SW limb is 08/340. The axial plane is 50/234. Post-folding strata show onlapping geometries above the anticline structure.

(B) The NW-SE Mugaire anticline

In the current cartographic configuration the most evident large scale folds in the southern margin of Bortziriak massif are E-W directed and eastward verging folds formed during the Alpine orogeny. Detailed restitution of Alpine deformation and stratigraphic configuration of Mesozoic materials reveals the existence of NNW-SSE oriented folds, formed during the Cretaceous (Fig. 4A). Five folds, with wavelengths up to some km, have been distinguished. The Mugaire fold is the best preserved and shows good evidence of its syn-sedimentary character.

The Mugaire anticline is a NW-SE oriented anticline (Fig. 7A), faulted by subparallel vertical and subvertical faults that coalesce in depth against Keuper lutites (Fig. 4A,B, Fig. 7B). The anticline was folded by the Alpine inversion, forming a E-W tight syncline (called the “Dépresion intérmediaire”; Lamare, 1936) resulting in the actual intersection with the topography, perpendicular to its axial plane (Fig. 7A). Folded pre-folding strata appear on top of basement rocks. Keuper materials showing variable thicknesses are present along the contact between the Palaeozoic/Triassic basement and pre-folding strata (Jurassic to Albian), indicating its play as a decoupling layer.

The SW limb dips 65º to the SW, and consists on a monoclinal block limited by the Bertiz and Oronoz faults that show syn-sedimentary activity during the Aptian and Albian. In the NE limb the pre-folding units are nearly parallel to post-folding Upper Cretaceous rocks (Fig. 7B). Almost the entire Azkorte Fm. of the hinge zone of the fold is eroded, with the exception of isolated outcrops (few metres thick) adjacent to faults and in the lowermost part of the anticline (Fig. 7A,B).

Post-folding strata overlie unconformably the pre-folding strata of the anticline. This unconformity is characterized by subaerial exposure and karstification features of the Buruntza limestones Fm. This surface represents the amalgamation of subsequent unconformities: the early late Albian U1 unconformity (Bodego et al., 2015) and U2. Locally, decimetric-sized outcrops of limestone breccia with sandy matrix (syn-folding Kostartzu Fm.) appear overlying the U1 surface (Fig. 8G,H). Moreover, limestone breccias also crop out interbedded with post-folding Upper Cretaceous marls that onlap the anticline.

(C) Restoration of the Mugaire faulted anticline

As in the previous cases, the datum considered for the structural restoration is the base of the Upper Cretaceous post-folding strata (Fig. 7D), dated as lower Cenomanian (Bodego et al., 2015). Since no data is available for the NE limb, we have considered pre-folding data of the adjacent SW block in order to calculate the axis of the anticline. Once restored to the horizontal (early Cenomanian), pre-folding strata of the SW limb show values of 71º dipping towards the SW (71/221) and the pre-folding strata of the adjacent SW block, 7º to the east (07/099). Thus, considering that the axial plane and axis of the anticline are parallel to those of the restored limbs (the adjacent syncline of the anticline), the orientation of the axial plane of the anticline is 34/214 and the axis is 06/133 (Fig. 7D).

The restored anticline structure shows that by the early Cenomanian the SW limb of the anticline rotated 71º by elevation of this limb, whereas the pre-folding strata to the SW of the Bertiz fault maintained subhorizontal (Fig. 7E). The thinned stratigraphic thickness due to erosion of the anticline structure and the post-folding strata unconformably overlying the anticline, indicate that this structure was formed by the early Cenomanian.

(A) DISCUSSION

The data presented above allow us to interpret the set of anticlines and synclines as extensional forced folds, formed by the combined action of basement faulting and salt mobilisation. This extensional forced folding can be inferred by: (i) the accumulation of salt below the anticlines nearby the fault and its extrusion through faults; (ii) the syn-folding resedimentation of pre-folding deposits at the foot of anticlines; (iii) onlap geometries of post-folding sediments; and iv) hardground features and neptunian dykes on unconformity surfaces.

(B) Latest Albian-early Cenomanian folding event

The dating of these structures is mainly based on (bio)stratigraphy and structural data. The datum to restore the structural data is the base of the Upper Cretaceous Calcareous flysch, because of its areal expansion and its apparent post-folding character unconformably overlying the Permian to lower Cenomanian strata. The base of this rock unit is diachronic in the Bortziriak massif margins, as shown by Bodego et al. (2015). In the NE margin, above the Errekalde anticline the base of the unit is latest early Cenomanian, whereas in the vicinity of the Txoritokieta anticline the age of this unit varies from Turonian to early Campanian, with an onlap geometry. In the southern margin, the base of the Upper Cretaceous calcareous flysch unit is also variable due to its onlapping character (Iriarte and Caron, 2003; Iriarte, 2004), but adjacent to the Mugaire anticline, the base of the unit has its oldest age, early Cenomanian.

Therefore, the structural restoration shows that anticline structures were already formed by the time of deposition of the Upper Cretaceous Calcareous flysch, although the diachronity due to an onlapping arrangement of the post-folding strata complicates the precise timing of the folding.

In the case of the Errekalde anticline, the timing is well constrained by the sedimentation of the Lasarte megabreccia Fm. (Bodego et al., 2008). The base is the U1 unconformity, which has progressive unconformity features close to the anticline (Fig. 5A), is dated latest Albian (*Stoliczkaia dispar* ammonite biozone) and indicates the beginning of the folding. The youngest rocks of the Lasarte Fm. are early Cenomanian, and the base of the Upper Cretaceous in the area is latest early Cenomanian (Fig. 2). Thus, this growth structure was active during at least the latest Albian to the early Cenomanian interval, for about 4 Ma. The progressive denudation of buried units is evidenced by the inverse stratigraphy of the syn-folding strata of the Lasarte megabreccia Fm. (Bodego et al., 2008, 2015). Upper Cretaceous deposits fossilized the structure indicating that no more folding occurred from latest early Cenomanian onwards.

No syn-folding deposits recording the growth of the Txoritokieta anticline have been recognized. Nevertheless, the differing facies and stratigraphic thicknesses of the Oiartzun Fm. in each limb suggests that by the late Albian-early Cenomanian the SW limb was a relatively uplifted block, with shallow marine carbonate platform sedimentation, whereas the northeast limb acted as a subsiding block registering a thick succession of thin- to coarse-grained coastal siliciclastics, intertongued with shallow-marine limestones from the Oiartzun Fm. (Fig. 2). The presence of pervasive planar neptunian dykes in the Oiartzun Fm. limestones (middle to lower part of the formation, not on the U2 surface) indicate that the carbonate platform fractured soon after its deposition and filled with sandy calcarenitic sediments and sand from above (from the Oiartzun Fm., Fig. 8E). We infer that fracturing was associated with extensional forced folding (Cosgrove and Ameen, 1999). Coherently with data above, onset of forced folding is dated at least at the late Albian.

The base of the Upper Cretaceous is diachronic over the anticline, drawing onlap geometries from the late Turonian to the early Campanian. This arrangement suggests that the anticline was probably formed by the late Turonian, and the topographic elevation was completely covered by the flysch sedimentation during the early Campanian. The development of a hardground on the top of Albian limestones (Fig. 8F) supports this hypothesis, since these features indicate that no sedimentation occurred during a long period of time. Thus, after its formation, the anticline structure was exposed on the marine seafloor over 6.2 Ma (Bodego et al., 2015).

In the southern margin, the Mugaire anticline features constrain the timing of the folding event. By the early Cenomanian, the SW limb was already rotated 71º. The erosion of the upper Albian to lower Albian (Azkorte and Buruntza Fms.) pre-folding strata and the presence of syn-folding (Kostartzu Fm.) deposits on top of U1 (Fig. 8G,H), indicate that during the late Albian to early Cenomanian, the anticline was still growing and progressively being eroded and resedimented in the lowest and deepest part of the anticline.

(B) Decoupling of deformation

(C) Extension and basement-fault propagation

For the Aptian-Cenomanian interval, extensional to transtensional strain controlled basement extension in the BCB, resulting in fault reactivation and basin compartmentalization (e.g. Martín-Chivelet et al., 2002; García-Mondéjar et al., 2004; Tugend et al., 2014). In the studied area, the syn-sedimentary activity of basement faults during the late Albian - early Cenomanian is evidenced by the stratigraphical (thickness, age, etc.) and sedimentological differences of the stratigraphic record across the Errekalde, Ereñozu, Leitza and Bertiz basement faults (Figs. 3 and 4). For instance, the Ereñozu fault controlled the sedimentation of the Oiartzun Fm. in its hanging-wall, whereas its footwall records very thin and isolated deposits (Fig. 3A,B).

The age and location of the forced folds above active extensional basement faults suggests that the anticline formation was controlled by the activity of basement extensional faults. The axes of the forced folds are NW-SE and E-W-trending, being parallel to inherited basement fault trends, reported all along the Pyrenean domain (e.g. Gisbert et al., 1983). Thus, the activity of these basement faults could have triggered the migration of Keuper deposits that deformed and faulted the overlying and detached Mesozoic cover resulting in forced folds and faults that accommodated the deformation. The reactivation of some of these basement faults was already accommodating basement extension since the late Aptian to late Albian, triggering thin-skinned tectonics above the same decoupling layer, the Upper Triassic Keuper clays and evaporites (Bodego and Agirrezabala, 2013).

(C) Decoupling layer, salt migration and anticline formation

The scenario presented for the Errekalde, Txoritokieta and Mugaire forced folds, includes interplay between extensional faulting within the sub-decollement basement and development of salt structures due to the presence of a ductile layer. The presence of Upper Triassic clays and evaporites is essential to understand the decoupling of extensional deformation into thin-skinned and basement (thick-skinned) extension.

Upward propagation of basement faults across weak layers can be inhibited (Withjack et al., 1990), resulting in a decoupling effect to accommodate sub-salt basement extension (Withjack et al., 1989, 1990; Stewart et al., 1997; Cosgrove and Ameen, 1999; Richardson et al., 2005; Ferrill et al., 2007). In the studied examples, Upper Triassic deposits separate the sub-decollement basement from Jurassic to Cretaceous deposits (supra-decollement or pre-folding strata) and acted as a decoupling layer controlling the upward propagation of extensional basement faults into the Mesozoic cover. Thus, the sub- and supra-decollement strata deformed in different ways under the same extensional stress.

The strain decoupling results in contrasting deformation between the basement and Mesozoic detached sedimentary successions. While extension is accommodated by brittle normal faults in the sub-salt basement, the supra-salt sedimentary succession or cover can accommodate the extension both by folding and stretching and/or faulting (Stearns, 1978; Brown, 1980; Laubscher, 1982; Withjack et al., 1989, 1990; Stewart et al., 1997; Cosgrove and Ameen, 1999; Richardson et al., 2005; Ferrill et al., 2007; Tavani and Granado, 2015).

In our studied cases folding and faulting of the supra-salt sedimentary cover can be attributed to both basement extension and subsequent salt migration. Basement faulting formed forced monoclinal folds in the Mesozoic cover and also differential subsidence, controlling the syn-folding sedimentation (and sedimentary loading) in different fault blocks (Figs. 5D, 6D, 7E). These processes triggered lateral and vertical salt flow (Vendeville and Jackson, 1992), especially in hanging-wall blocks and concentrated the salt along fault traces, like salt walls, causing the upward folding of the supra-decollement cover. However, the location of salt accumulation may not necessarily be located directly above the basement fault, since salt evacuation and inflation can be sourced both from the hangingwall and the footwall (e.g. Koyi et al. 1993; Burliga et al. 2012). In the study area, salt flow is evidenced by the presence of salt-cored anticlines, even with extrusion of Keuper rocks around or close to the hinge area, along hectometric to kilometric sized faults (e.g. Errekalde and Txoritokieta folds). We interpret that the salt extruded through faults that developed in order to accommodate the stretching due to the upward flow of the salt and bending. Although some of these faults could have been reactivated during the Alpine inversion, stratigraphic data indicate that these faults had already extruded Keuper rocks to the latest Albian - earliest Cenomanian seafloor. In the Txoritokieta faulted anticline, Keuper deposits along a small-scale fault are in stratigraphic contact (U2) with the overlying post-folding hemipelagic marls, indicating that by that time (probably early Cenomanian) Keuper materials had pierced the supra-salt cover and reached the seafloor.

Similarly, in the Errekalde fold, Keuper materials along the fault trace are overlain by syn-folding deposits.

The halokinetic processes invoked for the mid-Cretaceous continued, and even extruded to the sea bottom during the Late Cretaceous in most of the main basement faults limiting the rifting area in the BCB (Brinkmann and Lögters, 1968; Sappenfield and Schroeder, 1968; Pflug, 1967). The main diapirs and diapiric anticlines are nowadays located along the trace of that ancient basement faults, probably denoting the preferential migration of the decollement halokinetic layer towards them (wall-diapirism) since the Early Cretaceous (e. g. García-Mondéjar et al., 1996; Tavani et al., 2013; Tavani and Granado 2015, López-Horgue et al., 2010; Bodego and Agirrezabala, 2013; Poprawski et al., 2014, 2016).

(B) Evolution of the extensional folds of the Bortziriak Paleozoic massif margin

The study of the described syn-sedimentary forced folds allows depicting their evolution (Fig. 9).

Late Triassic. Keuper clays and evaporites deposited in a sabkha environment in the basin, overlying the basement, composed of Palaeozoic to Lower Triassic rocks (Fig. 9A).

Late Aptian to middle Albian. A major rift event occurred during this interval and basement extension provided the deposition of thick syn-rift sedimentary successions in the area. The viscous character of the decollement layer often prevented basement faults to propagate upwards into the sedimentary pile. This resulted in different stratigraphic thicknesses across basement faults: thicker successions registered in the subsiding blocks compared to thinner successions on the footwall blocks. Basement extension triggered halokinesis that evolved into salt walls (Fig. 9B).

Late Albian. The rise of the E-W and NW-SE trending salt walls was controlled by the activity of basement faults. The passive diapiric growth of the salt walls caused the inflation and tilting of the pre-folding strata above the faults. The growth of the anticlines caused the rotation and fracturing of pre-folding strata and fissures were filled with syn-folding sediments, resulting in neptunian dykes (Fig. 9C).

Latest Albian to early Cenomanian. The most intense period of diapiric rise created topographic highs. The increase in salt mobilization is attributed to a tectonic subsidence pulse related to an extensional rift phase. The newly created topographic reliefs were eroded, truncated and resedimented at the foot of the anticlines as breccias. Strain accommodation caused by the upward flow and bending produced faults that allowed extrusion of Keuper rocks to the seafloor (Fig. 9D).

Latest early Cenomanian to Turonian. The extensional phase ended and subsequently salt mobilization. The main forced fold formation phase stopped by the latest early Cenomanian, but small activity could have occurred, evidenced by syn-folding breccias interbedded within the post-folding strata. The basin underwent a general subsidence phase that caused the deepening of the study area and hemipelagic sediments fossilized the folds with onlap geometries at the toe of the folds (Fig. 9E).

Turonian to Campanian. The highest topographic projections of the folds were exposed on the seafloor during 6.2 Ma, where pervasive boring and iron oxide crust precipitation occurred. Hemipelagic sedimentation covered completely the structural reliefs by the Campanian (Fig. 9F).

(B) Folds in an extensional setting

Controversies about the mode of the opening of the Bay of Biscay - Pyrenean rift system during the Albian are still in debate. Interpretations based on geophysical data and field observations have apparently not been in accordance. Many authors, mainly based on field observations, invoke late Albian sinistral strike-slip in the BCB (Rat et al., 1983; García-Mondéjar, 1989;

García-Mondéjar et al., 1996; Iriarte, 2005) and also in the Pyrenean realm (Choukroune and Mattauer, 1978; Puigdefàbregas and Souquet, 1986; Olivet, 1986; Larrasoaña et al., 2003). In this context, some late Albian folds have been interpreted as transpressional to compressional structures in the BCB (García-Mondéjar et al., 1996; Agirrezabala et al., 2002; Quintanar-Soto, 2003) and also in the Pyrenean region (Choukroune, 1976; Debroas, 1978; Razin, 1989; Souquet and Peybernès, 1991; García-Senz, 2002).

On the contrary, recent studies invoke extreme crustal thinning due to N-S extension/hyperextension since the late Aptian until the early Cenomanian for the Bay of Biscay-BCB-Pyrenean realm (e.g. Jammes et al., 2009,2010; Lagabrielle et al., 2010; Roca et al., 2011; Tavani and Muñoz, 2012; Tugend et al., 2014; DeFelipe et al., 2017). Overall, the three examples presented show that the extensional folding phase occurred during the late Albian until the latest early Cenomanian. Examples of similar structures under extensional tectonics have been described for the Albian of the Parentis basin, considered a twin basin of the BCB of the Bay of Biscay realm (Ferrer et al., 2008, 2012, 2014). We propose that the above mentioned examples of the BCB could be reviewed to analyze if their compressive features could be explained by the extensional mechanism reported in this work. This would permit to advance in the discussion about the possible regional transpressional/compressional tectonic event in the BCB and in the Pyrenean realm during the latest Albian-early Cenomanian rifting, since here it is presented an alternative and more parsimonious extension-related mechanism to explain the growth of apparently compressional folds that support that assumption in a rift setting.

(A) CONCLUSIONS

Geological mapping around the Bortziriak-Cinco Villas Palaeozoic massif shows the presence of salt-cored folds. The tectonostratigraphic analysis of three of these anticlines demonstrates that the formation of these folds occurred during the late Albian to early Cenomanian and that they were fossilized by Cenomanian to Campanian strata.

The anticlines are located on top and parallel to inferred extensional syn-sedimentary basement faults, which Aptian − Cenomanian activity is evidenced by the stratigraphic record. The presence of an Upper Triassic viscous layer (Keuper) prevented the upward propagation of the normal basement faults into the sedimentary pile and acted as a decoupling layer between the rigid basement (Palaeozoic to Lower Triassic rocks) and the Mesozoic syn-rift sedimentary pile. However, this viscosity allowed the mobility of Keuper rocks that accumulated against the extensional basement faults as salt walls and caused the inflation of the strata above the faults generating salt-cored forced folds. The high mobility rates during the late Albian-early Cenomanian are attributed to high subsidence rates due to an extensional pulse.

The presence of sediment-filled fissures (neptunian dykes) on upper Albian strata evidences the progressive tilting of the folds. Similarly, faulting accommodated deformation of the pre-folding strata, allowing the extrusion of Keuper rocks to the seafloor by the early Cenomanian. The topographic projections created by the progressive inflation, tilting and folding of pre-folding strata were truncated, eroded and redeposited as syn-folding strata at the foot of the folds, since the late Albian until the early Cenomanian, when the main folding activity ceased.

Hemipelagic sedimentation fossilized the relative topographic highs with onlapping geometries and the highest topographic reliefs were completely covered by the Campanian.

The extensional origin of late Albian − early Cenomanian forced folds supports basement extension under pure extensional tectonics in the Basque-Cantabrian rift basin although arrangement and some features of the forced folds in the area may resemble transpressive deformation caused by strike-slip tectonics.

(A) ACKNOWLEDGMENTS

Stephano Tavani and an anonymous reviewer are thanked for valuable and constructive comments, which helped to improve the quality of the original manuscript. This research was funded by grant BFI05.398 from the Basque Government to A. Bodego and grant AP98-44159606 from the Spanish Science Ministry to E. Iriarte. Funds were also supplied by Ministerio de Educación y Ciencia (MEC) – Ministerio de Ciencia e Innovación (MICINN) (projects CGL2006-05491/BTE and CGL2009-08545) and Euskal Herriko Unibertsitatea (UPV/EHU) (projects EHU06/62, UNESCO06/03 and EHUA15/18).

(A) REFERENCES

Agirrezabala, L.M. , García-Mondéjar, J., 1989. Evolución tectosedimentaria de la plataforma urgoniana entre Cabo Ogoño e Itziar (Aptiense-Albiense superior, Región Vasco-Cantábrica Nor-Oriental). XII Congreso Español de Sedimentología. Simposio 11-20. Bilbao.

Agirrezabala, L.M., Owen, H.G. , García-Mondéjar, J. , 2002. Syntectonic deposits and punctuated limb rotation in an Albian submarine transpressional fold (Mutriku village, Basque-Cantabrian basin, northern Spain). Geol. Soc. Am. Bull. 114, 281-297.

Agirrezabala, L.M., Dinarès-Turell, J.,2013. Albian syndepositional block rotation and its geological consequences, Basque–Cantabrian Basin (western Pyrenees). Geol. Mag. 150(6), 986–1001. Doi: 10.1017/S0016756813000149.

Albarède, F., Michard-Vitrac, A., 1978. Age and significance of the north Pyrenean metamorphism. Earth Planet. Sci. Lett. 40(3), 327-332.

Badillo, T., 1982. Estudio geológico del sector de Ramales de la Victoria (prov. de Santander). Kobie. 12, 139-171.

Bodego, A., Iriarte, E., Agirrezabala, L.M., 2008. The deep-water Lasarte megabreccia (mid-Cretaceous, Basque-Cantabrian Basin): Sedimentological evidences of a growth structure denudation. Geo-Temas. 10, 1201-1204.

Bodego, A., Agirrezabala, L.M., 2013. Syn-depositional thin- and thick-skinned extensional tectonics in the mid-Cretaceous Lasarte sub-basin, western Pyrenees. Basin Res. 25(5), 594-612. Doi:10.1111/bre.12017.

Bodego, A., Iriarte, E., Agirrezabala, L. M., Garcia-Mondejar, J., Lopez-Horgue, M. A., 2015. Synextensional mid-Cretaceous stratigraphic architecture of the eastern Basque-Cantabrian basin margin (western Pyrenees). Cret. Res. 55, 229-261. Doi:10.1016/j.cretres.2015.01.006.

Boillot, G., Malod, J., 1988. The north and north-west Spanish continental margin: a review. Rev. Soc. Geol. España. 1(3-4), 295-316.

Brinkmann, R., Lögters, H., 1968. Diapirs in western Pyrenees and foreland, Spain, in: J. Braunstein, J., O´Brien, G. (Eds.), Diapirism and diapirs: a symposium. AAPG Mem. 8, 275-292.

Brown, R.N., 1980. History of exploration and discovery of Morgan, Ramadan, and July oilfields, Gulf of Suez, Egypt. Can. Soc. Pet. Geol. Mem. 6, 733-764.

Burliga, S., Koyi, H., Chemia, Z., 2012. Analogue and numerical modelling of salt supply to a diapiric structure rising above an active basement fault. Geol. Soc. Lond. Spec. Publ. 363, 395–408.

Camara, P., 1997. The Basque-Cantabrian basin´s Mesozoic tectono-sedimentary evolution, in: Bois, C., Gariel, O. (Eds.), Deep seismic study of the Earth´s crust: ECORS Bay of Biscay Survey, Mém. Soc. Géol. France, 171, 187-191.

Campos, J., 1979. Estudio geológico del Pirineo Vasco al W del río Bidasoa. Munibe. 31(1-2), 3-319.

Canérot, J., 1989. Rifting Eocrétacé et halocinèse sur la marge Ibérique des Pyrénées occidentales (France). Conséquences structurales. Bull. Centre Recherch. Pau-SNPA. 13, 87-99.

Canérot, J., Delavaux, F., 1986. Tectonics and sedimentation on the North-Iberian margin, chainons béarnaise South-Pyrenean zone (Pyrenees Basco-Bearnaises) – new data about the signification of the lherzolites in the Saraille area. C. R. Acad. Sc., Paris. 302 (15), 951-956.

Canérot, J., Lenoble, J.L.,1993. Diapirisme crétacé sur la marge ibérique des Pyrénées occidentales: exemple du pic de Lauriolle; comparaisons avec l'Aquitaine, les Pyrénées centrales et orientales. Bull. Soc. Géol. France. 164, 719-726.

Canérot, J., Hudec, M. R., Rockenbauch, K., 2005. Mesozoic diapirism in the Pyrenean orogen: Salt tectonics on a transform plate boundary. AAPG Bull. 89(2), 211-229.

Capote, R., Muñoz, J.A., Simón, J.L., Liesa, C.L., Arlegui, L.E., 2002. Alpine tectonics I: The Alpine system north of the Betic Cordillera, in: W. Gibbons, W., Moreno, M.T.(Eds.), Geology of Spain, Geological Society of London, pp. 385-397.

Choukroune, P.,1976. Structure et évolution tectonique de la zone nord-pyrénéenne. Analyse de la déformation dans une portion de la chaîne à schistosité subvertical. Mem. Soc. Géol. France. 127, pp. 116.

Choukroune, P., Mattauer, M.,1978. Tectonique des plaques et Pyrénées: Sur le fonctionnement de la faille transformante nord-pyrénéenne; comparison avec des modèles actuels. Bull. Soc. Géol. France. t. XX(nº 5), 689-700.

Cosgrove, J. W. , Ameen, M.S., 1999. A comparison of the geometry, spatial organization and fracture patterns associated with forced folds and buckle folds, in: Cosgrove, J.W., Ameen, M.S. (Eds.), Forced Folds and Fractures, Geol. Soc. Lond. Spec. Publ. 169, 7–21.

Debroas, E.J.,1978. Évolution de la fosse du flysch ardoisier de l'Albien supérieur au Sénonien inférieur (zone interne métamorphique des Pyrénées navarro-languedociennes). Bull. Soc. Géol. France. 7, 639-648.

De Felipe, I., Pedreira, D., Pulgar, J. A., Iriarte, E., Mendia, M.,2017. Mantle exhumation and metamorphism in the Basque□Cantabrian Basin (N Spain): Stable and clumped isotope analysis in carbonates and comparison with ophicalcites in the North□Pyrenean Zone (Urdach and Lherz). Geochem., Geophys.18(2), 631-652.

Ferrer, O., Roca, E., Benjumea, B., Muñoz, J. A., Ellouz, N., Marconi Team., 2008. The deep seismic reflection MARCONI-3 profile: Role of extensional Mesozoic structure during the pyrenean contractional deformation at the eastern part of the Bay of Biscay. Mar. Pet. Geol., 25(8), 714-730. Doi:http://dx.doi.org/10.1016/j.marpetgeo.2008.06.002.

Ferrer, O., Jackson, M. P. A., Roca, E., Rubinat, M., 2012. Evolution of salt structures during extension and inversion of the offshore parentis basin (eastern Bay of Biscay). Geol. Soc. Lond., Spec. Publ.. 363(1), 361-380. Doi:10.1144/SP363.16.

Ferrer, O., Roca, E., Vendeville, B. C., 2014. The role of salt layers in the hangingwall deformation of kinked-planar extensional faults: Insights from 3D analogue models and comparison with the parentis basin. Tectonophysics. 636, 338-350. Doi:http://dx.doi.org/10.1016/j.tecto.2014.09.013.

Ferrill, D.A., Morris, A.P., Smart, K.J., 2007. Stratigraphic control on extensional fault propagation folding: Big Brushy Canyon Monocline, Sierra Del Carmen, Texas, in: by Jolley, S.J., Barr, D., Walsh, J.J., Knipe, R.J.(Eds.), Structurally complex reservoirs, Geol. Soc. Lond. Spec. Publ. 292, 203–217.

Fort, X., Brun, J., P., Chuvel, F., 2004. Salt tectonics on the Angolan margin, synsedimentary deformation processes. AAPG Bull. 88 (11), 1523-1544.

García-Mondéjar, J., 1979. El complejo Urgoniano del sur de Santander. Unpublished phD thesis, UPV/EHU, 673 pp.

García-Mondéjar, J., 1982. Tectónica sinsedimentaria en el Aptiense y Albiense de la región vascocantábrica occidental. Cuadernos de Geología Ibérica. 8, 23-26.

García-Mondéjar, J.,1989. Strike-slip subsidence of the Basque-Cantabrian basin of the northern Spain and its relationship to Aptian-Albian opening of Bay of Biscay, in: Tankard, A.J., Balkwill, H.R. (Eds.), Extensional tectonics and stratigraphy of the North Atlantic margins. AAPG Mem. 46, 395-409.

García-Mondéjar, J. , García-Pascual, I., 1982. Estudio geológico del anticlinorio de Bilbao entre los ríos Nervión y Cadagua. Kobie.12, 101-137.

García-Mondejar, J., Robador, A.,1986-1987. Sedimentación y paleogeografía del Complejo Urgoniano (Aptiense-Albiense) en el area de Bermeo (region Vasco-Cantábrica septentional). Acta Geol. Hisp. t. 21-22, 411–418.

García-Mondéjar, J., Agirrezabala, L.M., Aranburu, A., Fernández-Mendiola, P.A., Gómez-Pérez, I., López-Horgue, M.A., Rosales, I.,1996. The Aptian-Albian tectonic pattern of the Basque-Cantabrian Basin (Northern Spain). Geol. J. 31, 13-45.

García-Mondéjar, J., Fernández-Mendiola, P.A., Agirrezabala, L.M., Aranburu, A., López-Horgue, M.A., Iriarte, E., Martínez-Rituerto, S., 2004. Extensión del Aptiense-Albiense en la Cuenca Vasco-Cantábrica, in: Vera, J.A.. (Ed.) Geología de España, Sociedad Geológica de España-Instituto Geológico y Minero de España, Madrid, pp. 340-343.

García-Senz, J., 2002. Cuencas extensivas del Cretácico Inferior en los Pirineos centrales: Formación y subsecuente inversión. Unpublished phD thesis, University of Barcelona, 310 pp.

Gisbert, J., Garúa, J.A., Gascón, F., Martí, J., Broutin, J., 1983. El Stephaniense-Pérmico del Pirineo Oriental. Cartografía, sedimentología, diagénesis y recursos de interés económico. Informe. Servei Geologic de la Generalitat de Catalunya, 114 p.

Heddebaut, C., 1973. Etudes géologiques dans les Massifs paléozoïques basques. Thèse Univ. ci. Tech. Lille. 272, 263 pp.

Heddebaut, C., 1975. Etudes géologiques dans les Massifs paléozoïques basques (résumé de thèse). Bull. B.R.G.M. IV, 1(2), 5-30.

Iriarte, E., 2004. La Depresión Intermedia entre Leitza y Elizondo (Pirineo occidental): estratigrafía y relaciones tectónica-sedimentación durante el Cretácico. Unpublished PhD thesis, UPV/EHU, 310 pp.

Iriarte, E., 2005. Tectosedimentary phases along the Leitza wrench fault related to Cretaceous Iberia/Europe plate boundary evolution. International Conference on Tectonics of Strike-slip: Restraining and Releasing bends in Continental and oceanic settings. Geological Society of London, London.

Iriarte, E., Caron, M., 2003. Edad de los términos basales del Cretácico Superior de la Depresión Intermedia (Pirineos occidentales, Nafarroa). Geogaceta. 34, 71-74.

Jammes, S., Manatschal, G., Lavier, L., Masini, E., 2009. Tectonosedimentary evolution related to extreme crustal thinning ahead of a propagating ocean: example of the western Pyrenees. Tectonics. 28, TC4012.

Jammes, S., Manatschal, G., Lavier, L., 2010. Interaction between prerift salt and decollement faulting in hyperextended rift systems: The example of the Parentis and Mauléon basins (Bay of Biscay and western Pyrenees). AAPG Bulletin. 94, 957-975.

Koyi, H., Jenyon, M. K., Peterson, K., 1993. The effect of basement faulting on diapirism. J. Pet. Geol. 16, 285–312.

Lagabrielle, Y., Bodinier, J., 2008. Submarine reworking of exhumed subcontinental mantle rocks: field evidence from the Lherz peridotites, French Pyrenees. Terra Nova. 20, 11-21.

Lagabrielle, Y., Labaume, P., De Saint Blanquat, M., 2010. Mantle exhumation, crustal denudation, and gravity tectonics during Cretaceous rifting in the Pyrenean realm (SW Europe): Insights from the geological setting of the lherzolite bodies. Tectonics. 29, TC4012.

Lamare, P., 1936. Recherches gèologiques dans les Pyrénees basques d'Espagne. Mem. Soc. Géol. Fr. 27.

Larrasoaña, J.C. , Parés, J.M., Millán, H., Del Valle, J., Pueyo, E.L., 2003. Paleomagnetic, structural and stratigraphic constraints on transverse fault kinematics during basin inversion: the

Pamplona Fault (Pyrenees, N Spain), Tectonics. 22(6), 1071, 10-22. Doi:10.1029/2002/TC001446.

Laubscher, H. P., 1982. Die Sudostecke des Rheingrabens-ein kinematisches und dynamisches problem. Eclogae Geol. Helv. 75, 101-116.

Lewis, M. M., Jackson, C. A., Gawthorpe, R. L., 2013. Salt-influenced normal fault growth and forced folding: The Stavanger fault system, North Sea. J.Struct. Geol. 54, 156-173. Doi:http://dx.doi.org/10.1016/j.jsg.2013.07.015

López-Horgue, M. A., Iriarte, E., Schroeder, S., Fernández-Mendiola, P. A., Caline, B., Corneyllie, H., Frémont, J., Sudrie, M., Zerti, S., 2010. Structurally controlled hydrothermal dolomites in Albian carbonates of the ason valley, basque cantabrian basin, northern Spain. Mar. Pet. Geol. 27(5), 1069-1092. Doi:10.1016/j.marpetgeo.2009.10.015

Martín-Chivelet, J., Berastegui, X., Rosales, I., Vilas, L., Vera, J.A., Caus, E., Gräfe, K., Mas, R., Puig, C., Segura, M., Robles, S., Floquet, M., Quesada, S., Ruiz-Ortiz, P.A., Fregenal-Martínez, M.A., Salas, R., Arias, C., García, A., Martín-Algarra, A., Melendez, M.N., Chacón, B., Molina, J.M., Sanz, J.L., Castro, J.M., García-Gernández, M., Carenas, B., García-Hidalgo, J., Gil, J., Ortega, F., 2002. Cretaceous, in: Ed. by W. Gibbons, W., Moreno, M.T. (Eds.), The Geology of Spain. The Geological Society, London, pp-255-292.

Martín-Martín, J. D., Vergés, J., Saura, E., Moragas, M., Messager, G., Baqués, V.,Razin, P., Grélaud, C., Malaval, M., Joussiaume, R.,Casciello, E.,Cruz-Orosa, I., Hunt, D. W., 2016. Diapiric growth within an Early Jurassic rift basin: The Tazoult salt wall (central High Atlas, Morocco). Tectonics. 36, 2-32. Doi:10.1002/2016TC004300.

Maurin, J.-C., Nivière, B., 2000. Extensional forced folding and décollement of the pre-rift series along the Rhine Graben and their influence on the geometry of the syn-rift sequences. Geological Society, London, Special Publications. 169, 73-86.

Mathey, B., 1987. Les flyschs cretacé supérieur des Pyrénées basques: age, anatomie, origine du matériel milieu de dépot et relations avec l'ouvert du Golfe de Gascogne. Memoires Géologique de l'Université de Dijon. 12, 402.

Mendia, M., Gil-Ibarguchi, J., 1991. High-grade metamorphic rocks and peridotites along the Leiza fault (western Pyrenees, Spain). Geol. Rundsch. 80(1), 93-107. Doi:10.1007/BF01828769.

Montadert, L., Roberts, D.G., De Charpal, O., Guennoc, P., 1979. Rifting and subsidence of the northern continental margin of the Bay of Biscay. Initial reports of the Deep Sea Drilling Project, Leg 48, Brest, France to Aberdeen, Scotland, 1976. Sripps Institution of Oceanography, UK distributors IPOD Committee, NERC, Swindon, pp. 1025-1060.

Morley, C.K., Guerin, G., 1996. Comparison of gravity-driven deformation styles and behavior associated with mobile shales and salt. Tectonics. 15 (6), 1154-1170.

Olivet, J.L.,1996. Kinematics of the Iberian Plate. Bull. Centre. Rech. Expl.-Prod. Elf Aquitaine. 20, 131-195.

Pascoe, R., Hooper, R., Storhaug, K., Harper, H., 1999. Evolution of extensional styles at the southern termination of the Nordland Ridge, Mid-Norway: a response to variations in coupling above Triassic salt. in: Ed. by A.J. Fleet, A.J., Boldy, S.A.R. (Eds.), Petroleum Geology of Norwest Europe: Proceedings of the 5th Conference. Geological Society, London, pp. 83-90. Doi:https://doi.org/10.1144/0050083.

Pflug, R., 1967. Der Diapir von Estella (Nordspanien). Beih. Geol. Jb. 66, 21-62.

Poprawski, Y., Basile, C., Agirrezabala, L. M., Jaillard, E., Gaudin, M., Jacquin, T., 2014. Sedimentary and structural record of the Albian growth of the Bakio salt diapir (the Basque Country, northern Spain). Basin Res. 26(6), 746-766. Doi:10.1111/bre.12062.

Poprawski, Y., Christophe, B., Etienne, J., Matthieu, G., Michel, L., 2016. Halokinetic sequences in carbonate systems: An example from the middle Albian Bakio breccias formation (Basque Country, Spain). Sediment. Geol. 334, 34-52. Doi:http://dx.doi.org/10.1016/j.sedgeo.2016.01.013.

Puigdefàbregas, C., Souquet, P., 1986. Tecto-sedimentary cycles and depositional sequences of the Mesozoic and Tertiary from the Pyrenees. Tectonophysics. 129, 173-203.

Quintanar-Soto, A.B., 2003. El Cretácico medio del extremo suroriental del Anticlinorio de Bilbao: Estratigrafía y Sedimentología. Unpublished phD thesis, UPV/EHU, 217 pp.

Rat, P., 1959. Les pays crétacés basco-cantabriques (Espagne). Thèse doctoral Université de Dijon. 18, 525 pp.

Rat, P., Amiot, M., Feuillée, P., Floquet, M., Mathey, B., Pascal, A., Salomon, J., 1983. Vue sur le Crétacé basco-cantabrique et nord-ibérique. Mém. Géol. Univ. Dijon. 9, 1-191.

Ravier, J., 1959. Le métamorphisme des terrains secondaires des Pyrénées. Mem. Soc. géol. Fr. XXXVIII, 2-3, 86, 250 p.

Razin, P., 1989. Évolution tecto-sédimentaire alpine des Pyrénées Basques a l'ouest de la transformante de Pamplona (Province du Labourd). Thèse doctoral Université de Bordeaux III, 464 pp.

Requadt, H., 1974. Aperçu sur la stratigraphie et le facies du Devonien inferieur et le moyen dans les Pyrénées Occidentales d'Espagne. Pirineos. 111, 109-127.

Richardson, N. J., Underhill, J. R., Lewisw, G., 2005. The role of evaporite mobility in modifying subsidence patterns during normal fault growth and linkage, Halten Terrace, Mid-Norway. Basin Res. 17, 203–223. Doi:10.1111/j.1365-2117.2005.00250.x.

Roca, E., Muñoz, J.A., Ferrer, O., Ellouz, N., 2011. The role of the Bay of Biscay Mesozoic extensional structure in the configuration of the Pyrenean orogen: Constraints from the MARCONI deep seismic reflection survey. Tectonics. 30, TC2001.

Sappenfield, L.W., Scroeder, E.R., 1968. Iza, an unusual diapir in northern Spain, in: Braunstein, J., O´Brien, G. (Eds.), Diapirism and diapirs: a symposium. Am. Assoc. Pet. Geol. Mem. 8, 293-300.

Serrano, A., Martínez Del Olmo, W., 2004. Estructuras diapíricas de la zona meriodional de la Cuenca Vasco-Cantábrica, in: Vera, J.A. (Ed.), Geología de España. Sociedad Geológica de España – Instituto Geológico y Minero de España, pp. 334-338.

Sharp, I. R., Gawthorpe, R. L., Underhill, J. R., Gupta, S., 2000. Fault-propagation folding in extensional settings: Examples of structural style and synrift sedimentary response from the Suez rift, Sinai, Egypt. Geol. Soc. Am. Bull. 112(12), 1877-1899. Doi:10.1130/0016-7606(2000)112<1877:FPFIES>2.0.CO;2.

Soler y José, R., 1972. El Jurásico y Cretáceo inferior de Leiza y Tolosa (Cuenca Cantábrica Oriental). Bol. Geol. Min. 83(6), 582-594.

Souquet, P., Peybernès, B., 1991. Stratigraphie séquentielle du cycle Albien dans les Pyrénées Franco-Espagnoles. Bull. Cent. Rech. Pau-SNPA. 15, 195-213.

Stearns, D. W., 1978. Faulting and forced folding in the Rocky Mountains foreland. Geol. Soc. Am. Mem. 151, 1-38.

Stewart, S.A., Ruffell, A.H., Harvey, M.J., 1997. Relationship between basement-linked and gravity-driven fault systems in the UKCS salt basins. Mar. Pet. Geol. 14(5), 581-604.

Tavani, S., Muñoz, J.A., 2012. Mesozoic rifting in the Basque-Cantabrian Basin (Spain): Inherited faults, transversal structures and stress perturbation. Terra Nova. 24, 70–76. Doi:10.1111/j.1365-3121.2011.01040.x.

Tavani, S., Carola, E., Granado, P., Quintà, A., Muñoz, J. A., 2013. Transpressive inversion of a Mesozoic extensional forced fold system with an intermediate décollement level in the Basque-Cantabrian basin (Spain). Tectonics. 32(2), 146-158. Doi:10.1002/tect.20019.

Tavani, S., Granado, P., 2015. Along-strike evolution of folding, stretching and breaching of supra-salt strata in the Plataforma Burgalesa extensional forced fold system (northern Spain). Basin Res. 27(4), 573-585. Doi:10.1111/bre.12089.

Tugend, J., Manatschal, G., Kusznir, N. J., Masini, E., Mohn, G., Thinon, I., 2014. Formation and deformation of hyperextended rift systems: Insights from rift domain mapping in the Bay of Biscay-Pyrenees. Tectonics. 33(7), 1239-1276. Doi:10.1002/2014TC003529.

Tvedt, A.B.M., Rotevatn, A., Jackson, C. A., Fossen, H., Gawthorpe, R. L., 2013. Growth of normal faults in multilayer sequences: A 3D seismic case study from the Egersund Basin, Norwegian North Sea. J. Struct. Geol. *55*, 1-20.

Vendeville, B.C, Jackson, M.P.A., 1992. The rise of diapirs during thin-skinned extension. Mar. Pet. Geol. 9(4), 331-354.

Wilson, P., Elliott, G. M., Gawthorpe, R. L., Jackson, C. A., Michelsen, L., Sharp, I.R., 2013. Geometry and segmentation of an evaporite-detached normal fault array: 3D seismic analysis of the southern Bremstein fault complex, offshore mid-Norway. J. Struct. Geol. 51, 74-91. Doi: http://dx.doi.org/10.1016/j.jsg.2013.03.005.

Withjack, M. O., Callaway, S., 2000. Active normal faulting beneath a salt layer: an experimental study of deformation patterns in the cover sequence. AAPG Bull. 84(5), 627-651.

Withjack, M. O., Meisling, K., Russell, L., 1989. Forced folding and basement-detached normal faulting in the Haltenbanken area, offshore Norway, in: Tankard, A.J., Balkwill, H.R. (Eds.), Extensional Tectonics and Stratigraphy of the North Atlantic Margins, AAPG Mem. 46, 567–575.

Withjack, M.O., Olson, J., Peterson, E., 1990. Experimental models of extensional forced folds. AAPG Bull. 74, 1038-1054.

(A) FIGURE CAPTIONS

Figure 1. A) Synthetic map of the Pyrenees with indication of the westernmost Palaeozoic massifs. B) Geological map of the westernmost Pyrenees with an indication of the study area (NW and S margins of the Bortziriak – Cinco Villas Palaeozoic massif).

Figure 2. Synthetic stratigraphic column with description of the general stratigraphy and sedimentology of the study area. Strata are divided into five major strata groups based on their relationship with the late Albian −early Cenomanian tectonic event and decollement layer. U1 corresponds to a latest Albian discontinuity with disconformity, angular unconformity and progressive angular unconformity features. U2 corresponds to an early Cenomanian−late Campanian discontinuity defined by the diachronous onlap of the Calcareous Flysch on mid-Cretaceous rocks, with low- to high-angle unconformity features.

Figure 3. A) Geological map of the NW margin of the study area. B) Reconstruction of the structural pattern for late Albian-early Cenomanian of the NW margin.

Figure 4. A) Geological map of the S margin of the study area. B) Reconstruction of the structural pattern for late Albian-early Cenomanian of the S margin.

Figure 5. A) Detailed geological map of the Errekalde anticline area with location of cross-section A-A' in B. B) Present day interpretative N-S to NW-SE cross-section (A-A') of the Errekalde anticline. Inset: equal-area stereographic projection of poles of pre- and post-folding strata. C) Stratigraphic column of the southern and northern limbs of the Errekalde fold. D) Interpretative tectono-stratigraphic architecture of the Errekalde anticline for the early-middle Cenomanian. Inset: equal-area stereographic projections of poles of pre- and post-folding strata restored to datum and resulting mean limb, axial plane and axis orientations.

Figure 6. A) Detailed geological map of the Txoritokieta anticline area with location of cross-section A-A' in B. B) Present day interpretative SW-NE cross-section (A-A') of the Txoritokieta anticline. Inset: equal-area stereographic projection of poles of pre- and post-folding strata. C) Stratigraphic column of the NE and SW limbs of the Txoritokieta fold. D) Interpretative tectono-stratigraphic architecture of the Txoritokieta anticline for the Campanian. Inset: equal-area stereographic projections of poles of pre- and post-folding strata restored to datum and resulting mean limb, axial plane and axis orientations.

Figure 7. A) Detailed geological map of the Mugaire anticline area. B) Present day interpretative SW-NE cross-section (A-A') of the Mugaire anticline. Inset: equal-area stereographic projection of poles of pre- and post-folding strata. C) Stratigraphic column of the SW and NE limbs of the Mugaire fold and the adjacent Oieregi trough to the west of the Bertiz fault. D) Equal-area stereographic projections of poles of pre- and post-folding strata restored to datum and resulting mean limb, axial plane and axis orientations. E) Interpretative tectono-stratigraphic architecture of the Mugaire anticline for the Campanian.

Figure 8. Field photographs of Txoritokieta and Mugaire forced folds. A) Outcrop photograph of the contact between pre-folding (Oiartzun Fm. limestones) and post-folding marls (with indication of U2) on the SW limb of the Txoritokieta anticline. B) Outcrop photograph of the contact between pre-folding (Oiartzun Fm. limestones) and post-folding marls (with indication of U2) on the NE limb of the Txoritokieta anticline. C) Outcrop photograph of the contact (U2) between the post-folding marls and the Keuper deposits on the Txoritokieta anticline. D) Detail of the U2 surface on the SW limb of the Txoritokieta anticline: Planar fissures of the top are filled with post-folding marls from above. E) Fracture in the Oiartzun Fm. limestones (pre-folding strata) filled with sandy calcarenites from the Oiartzun Fm. (neptunian dyke), Txoritokieta anticline. F) Detail of the U2 surface on the NE limb of the Txoritokieta anticline with pervasive borings, hardground features and ferruginous crusts. Post-folding marls appear onlapping the Oiartzun Fm. limestones. G and H) Outcrop photographs of Kostartzu Fm.

breccias, compound by Aptian Albian heterometric limestone (Buruntza Fm.) clasts and sandy matrix.

Figure 9. Schematic evolutionary model of the extensional forced folds around the Bortziriak – Cinco Villas massif. Main evolutionary diapiric stages and ages are illustrated with reference to basement, decollement layer, pre-folding, syn-folding and post-folding strata. The model is not to scale and represents a synthesis of the data observed in the Errekalde, Txoritokieta and Mugaire forced folds.

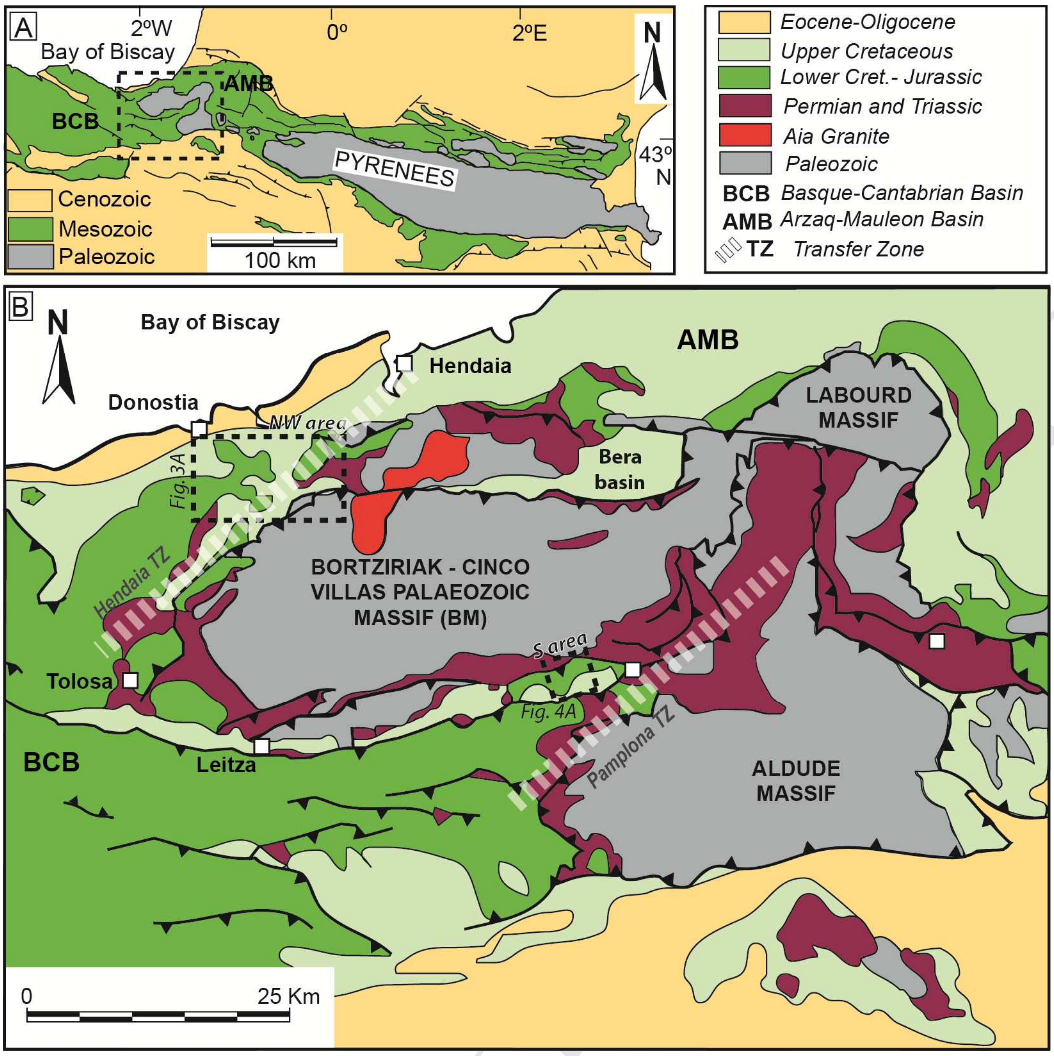
A
2ºW
0º
2ºE
N
Bay of Biscay
AMB
BCB
PYRENEES
43º N
Cenozoic
Mesozoic
Paleozoic
100 km
Eocene-Oligocene
Upper Cretaceous
Lower Cret.- Jurassic
Permian and Triassic
Aia Granite
Paleozoic
BCB Basque-Cantabrian Basin
AMB Arzaq-Mauleon Basin
TZ Transfer Zone
B
N
Bay of Biscay
Hendaia
AMB
Donostia
NW area
LABOURD MASSIF
Bera basin
Fig. 3A
Hendaia TZ
BORTZIRIAK - CINCO VILLAS PALAEOZOIC MASSIF (BM)
S area
Tolosa
Fig. 4A
Pamplona TZ
BCB
Leitza
ALDUDE MASSIF
0
25 Km

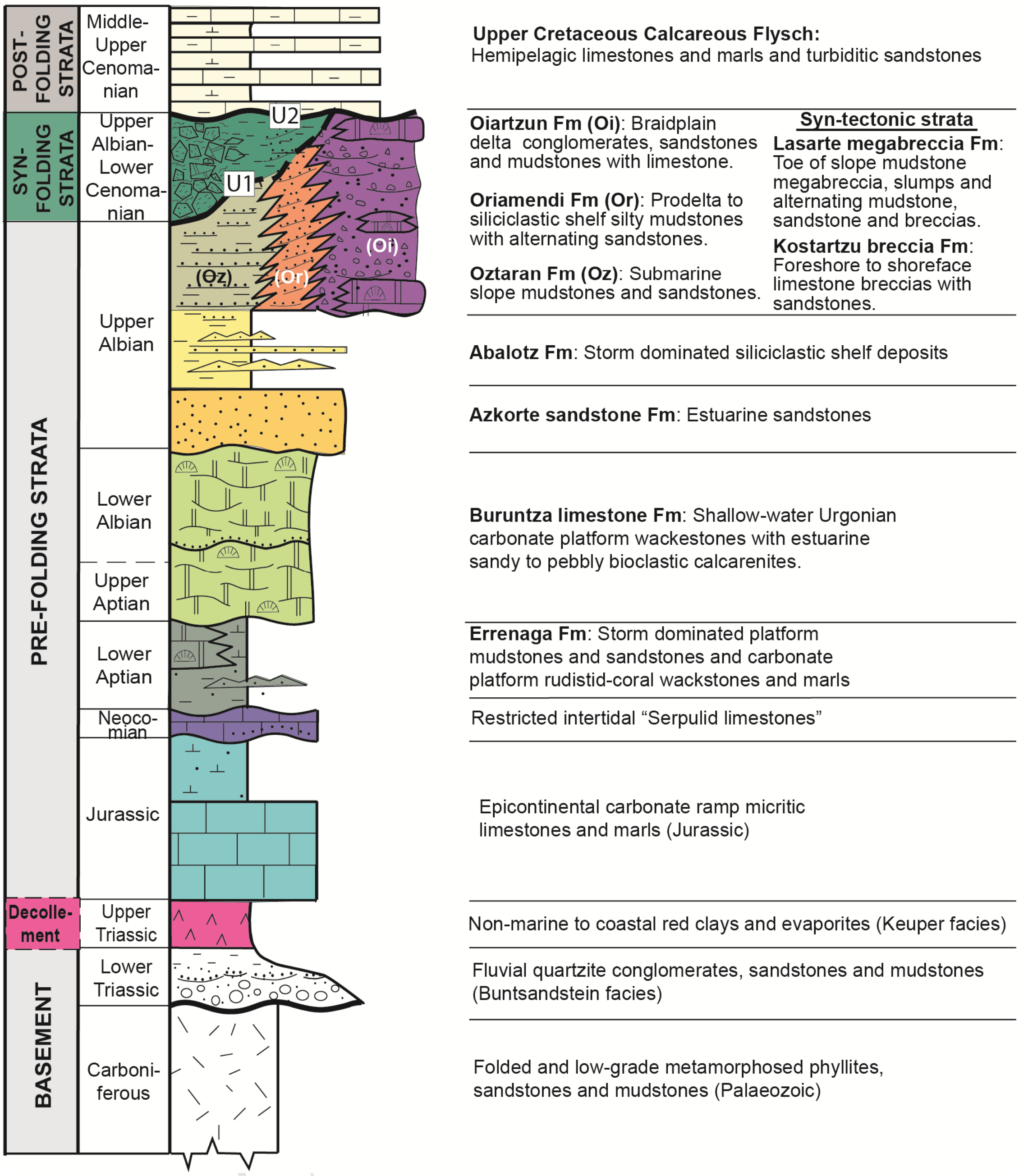

POST-FOLDING STRATA
SYN-FOLDING STRATA
PRE-FOLDING STRATA
Decolle-ment
BASEMENT
Middle-Upper Cenomanian
Upper Albian-Lower Cenomanian
Upper Albian
Lower Albian
Upper Aptian
Lower Aptian
Neocomian
Jurassic
Upper Triassic
Lower Triassic
Carboniferous
U2
U1
(Oz)
(Or)
(Oi)
Upper Cretaceous Calcareous Flysch: Hemipelagic limestones and marls and turbiditic sandstones
Oiartzun Fm (Oi): Braidplain delta conglomerates, sandstones and mudstones with limestone.
Oriamendi Fm (Or): Prodelta to siliciclastic shelf silty mudstones with alternating sandstones.
Oztaran Fm (Oz): Submarine slope mudstones and sandstones.
Syn-tectonic strata
Lasarte megabreccia Fm: Toe of slope mudstone megabreccia, slumps and alternating mudstone, sandstone and breccias.
Kostartzu breccia Fm: Foreshore to shoreface limestone breccias with sandstones.
Abalotz Fm: Storm dominated siliciclastic shelf deposits
Azkorte sandstone Fm: Estuarine sandstones
Buruntza limestone Fm: Shallow-water Urgonian carbonate platform wackestones with estuarine sandy to pebbly bioclastic calcarenites.
Errenaga Fm: Storm dominated platform mudstones and sandstones and carbonate platform rudistid-coral wackestones and marls
Restricted intertidal “Serpulid limestones”
Epicontinental carbonate ramp micritic limestones and marls (Jurassic)
Non-marine to coastal red clays and evaporites (Keuper facies)
Fluvial quartzite conglomerates, sandstones and mudstones (Buntsandstein facies)
Folded and low-grade metamorphosed phyllites, sandstones and mudstones (Palaeozoic)

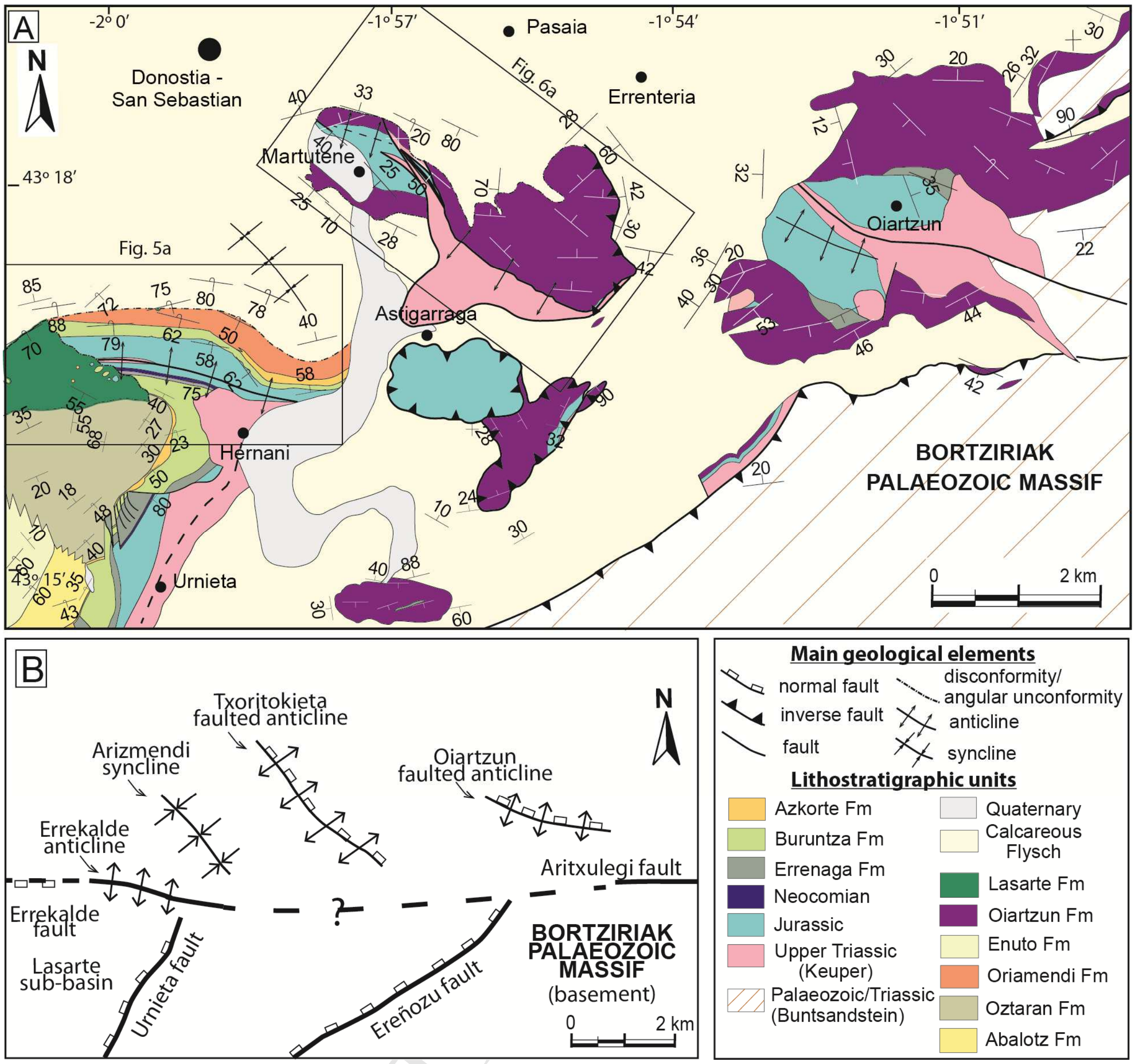
A
N
Donostia -
San Sebastian
Pasaia
Errenteria
Martutene
Oiartzun
Astigarraga
Hernani
Urnieta
Fig. 5a
Fig. 6a
-2° 0′
-1° 57′
-1° 54′
-1° 51′
43° 18′
43° 15′
BORTZIRIAK
PALAEOZOIC MASSIF
0
2 km
B
Txoritokieta
faulted anticline
Arizmendi
syncline
Oiartzun
faulted anticline
Errekalde
anticline
Aritxulegi fault
Errekalde
fault
Lasarte
sub-basin
Urnieta fault
Ereñozu fault
BORTZIRIAK
PALAEOZOIC
MASSIF
(basement)
Main geological elements
normal fault
inverse fault
fault
disconformity/
angular unconformity
anticline
syncline
Lithostratigraphic units
Azkorte Fm
Buruntza Fm
Errenaga Fm
Neocomian
Jurassic
Upper Triassic
(Keuper)
Palaeozoic/Triassic
(Buntsandstein)
Quaternary
Calcareous
Flysch
Lasarte Fm
Oiartzun Fm
Enuto Fm
Oriamendi Fm
Oztaran Fm
Abalotz Fm

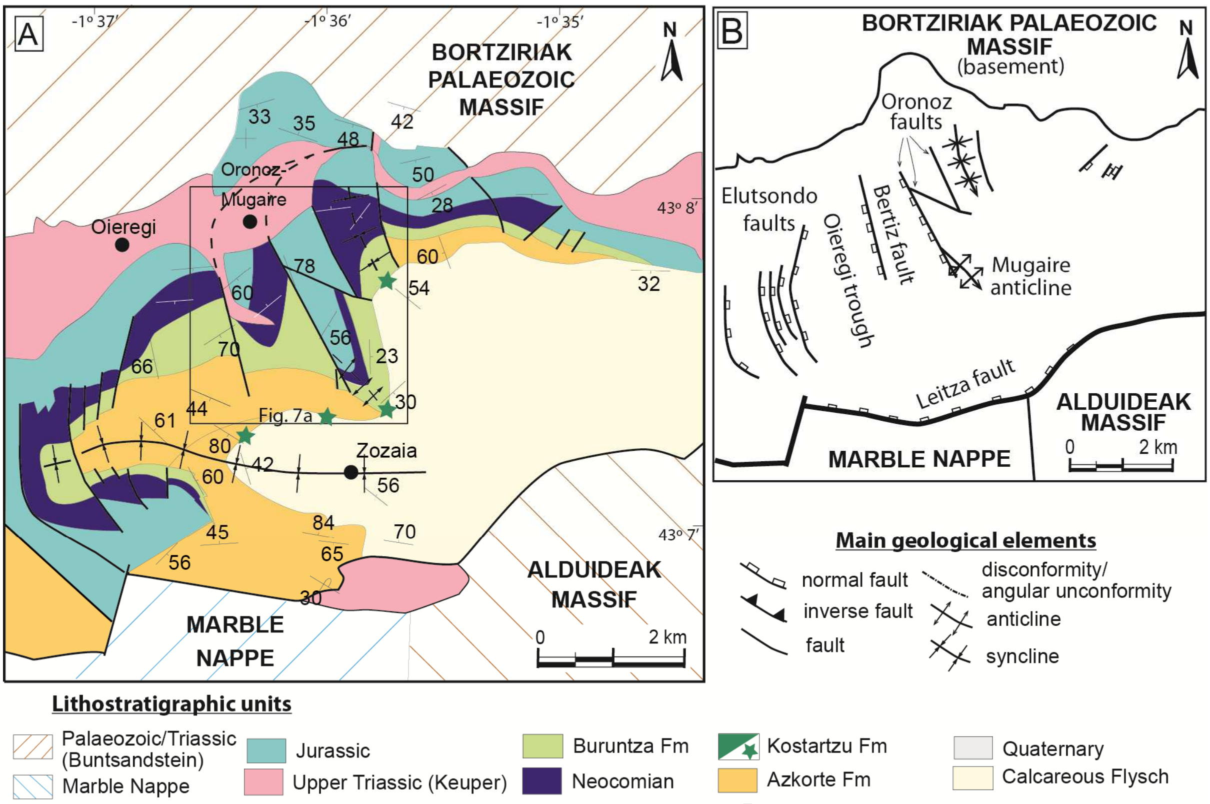
A
-1° 37′
-1° 36′
-1° 35′
N
BORTZIRIAK PALAEOZOIC MASSIF
Oronoz-Mugaire
Oieregi
Fig. 7a
Zozaia
43° 8′
43° 7′
ALDUIDEAK MASSIF
MARBLE NAPPE
0
2 km
B
BORTZIRIAK PALAEOZOIC MASSIF
(basement)
Oronoz faults
Elutsondo faults
Oieregi trough
Bertiz fault
Mugaire anticline
Leitza fault
ALDUIDEAK MASSIF
MARBLE NAPPE
Main geological elements
normal fault
inverse fault
fault
disconformity/ angular unconformity
anticline
syncline
Lithostratigraphic units
Palaeozoic/Triassic (Buntsandstein)
Marble Nappe
Jurassic
Upper Triassic (Keuper)
Buruntza Fm
Neocomian
Kostartzu Fm
Azkorte Fm
Quaternary
Calcareous Flysch

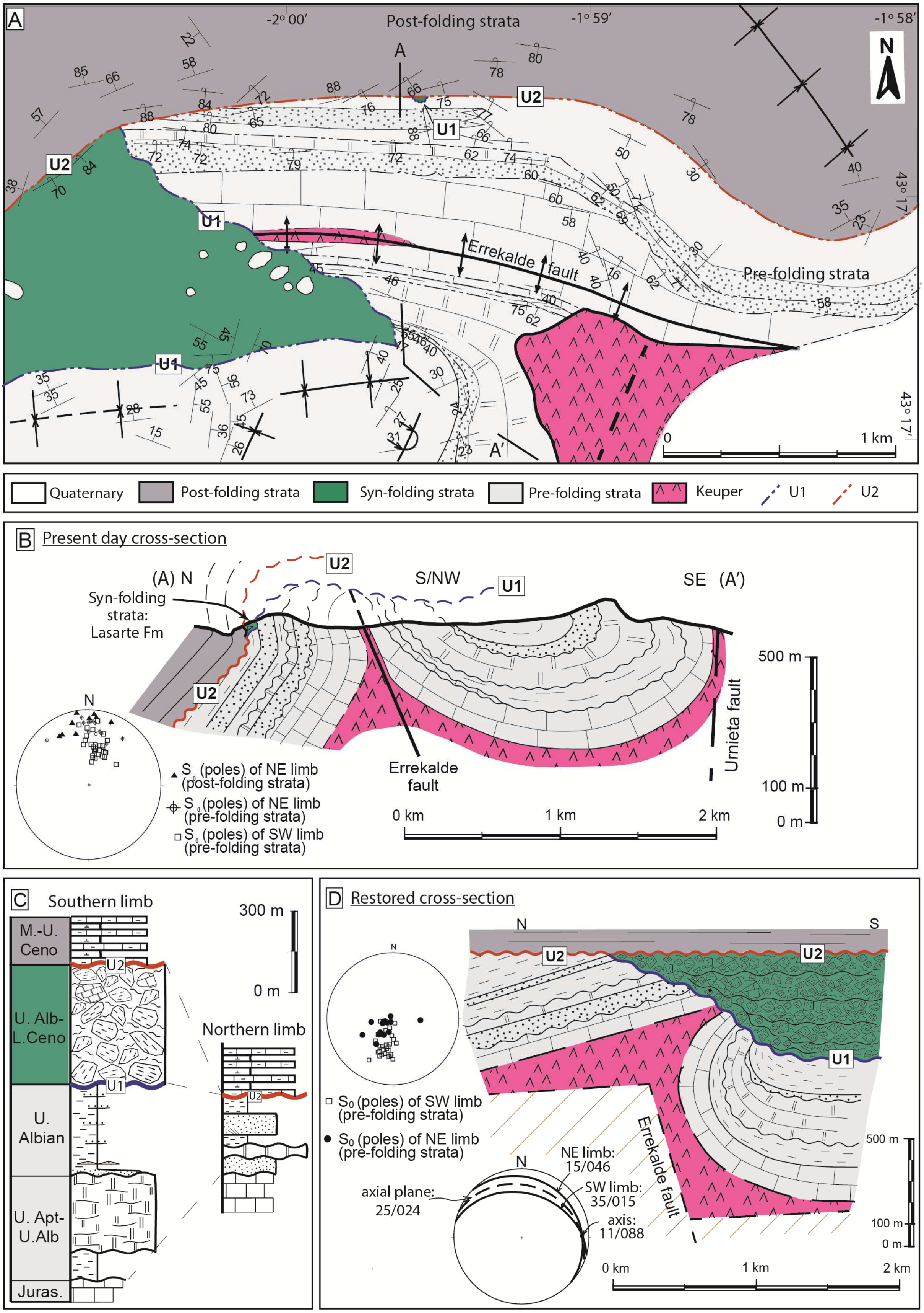
A
-2° 00′
Post-folding strata
-1° 59′
-1° 58′
N
A
U2
U1
U2
U1
U1
Errekalde fault
Pre-folding strata
43° 17′
43° 17′
A′
0
1 km
Quaternary
Post-folding strata
Syn-folding strata
Pre-folding strata
Keuper
U1
U2
B
Present day cross-section
(A) N
S/NW
SE (A′)
Syn-folding strata: Lasarte Fm
U2
U1
U2
500 m
100 m
0 m
Urnieta fault
Errekalde fault
0 km
1 km
2 km
N
S0 (poles) of NE limb (post-folding strata)
S0 (poles) of NE limb (pre-folding strata)
S0 (poles) of SW limb (pre-folding strata)
C
Southern limb
300 m
0 m
M.-U. Ceno
U2
U. Alb-L.Ceno
U1
U. Albian
U. Apt-U.Alb
Juras.
Northern limb
U2
D
Restored cross-section
N
S
U2
U2
U1
N
S0 (poles) of SW limb (pre-folding strata)
S0 (poles) of NE limb (pre-folding strata)
Errekalde fault
N
NE limb: 15/046
SW limb: 35/015
axis: 11/088
axial plane: 25/024
500 m
100 m
0 m
0 km
1 km
2 km

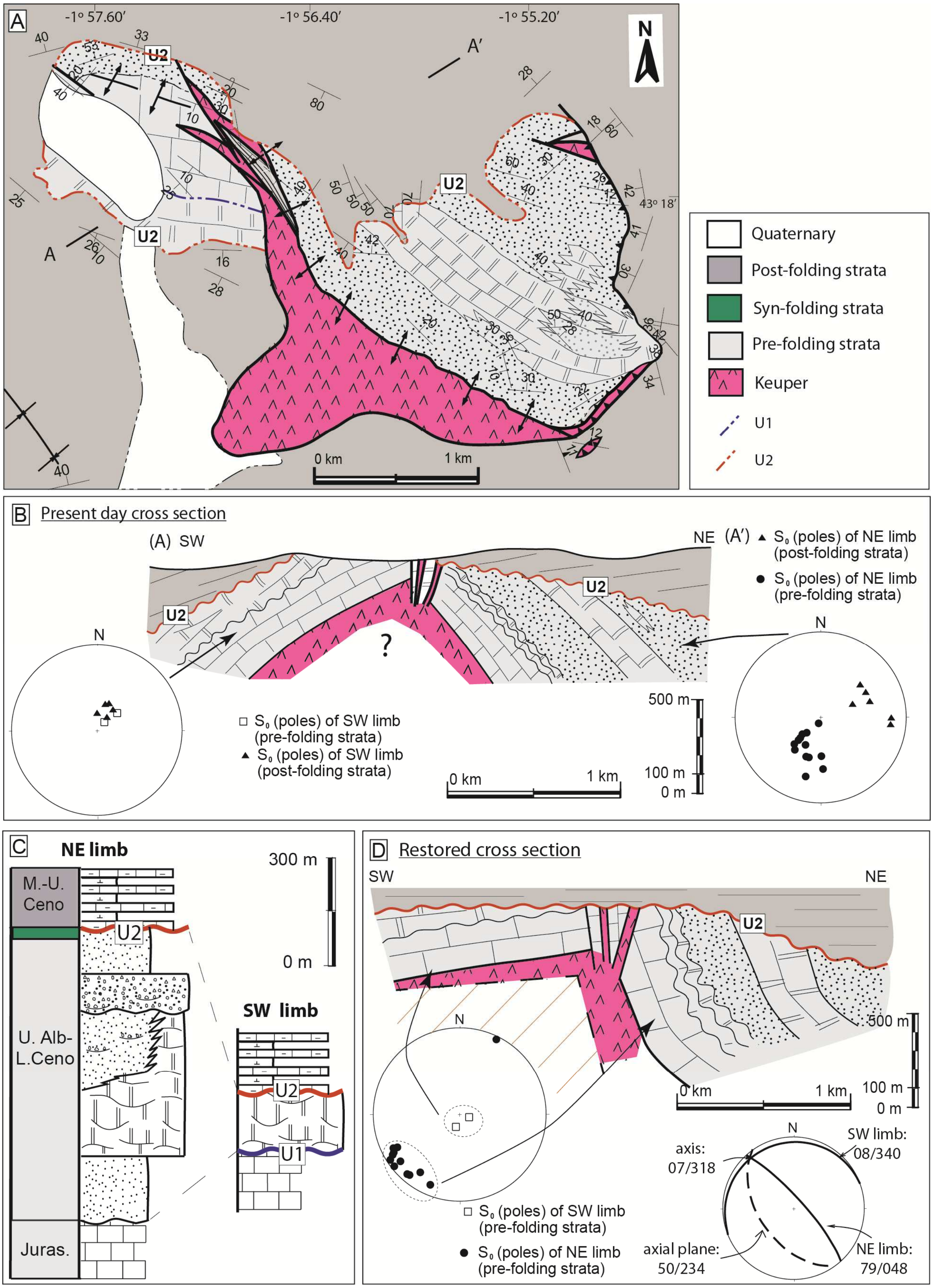
A
-1° 57.60′
-1° 56.40′
-1° 55.20′
N
A′
A
U2
43° 18′
0 km
1 km
Quaternary
Post-folding strata
Syn-folding strata
Pre-folding strata
Keuper
U1
U2
B
Present day cross section
(A) SW
NE (A′)
S₀ (poles) of NE limb (post-folding strata)
S₀ (poles) of NE limb (pre-folding strata)
S₀ (poles) of SW limb (pre-folding strata)
S₀ (poles) of SW limb (post-folding strata)
500 m
100 m
0 m
C
NE limb
M.-U. Ceno
U. Alb-L.Ceno
Juras.
300 m
0 m
SW limb
U1
D
Restored cross section
SW
NE
axis: 07/318
SW limb: 08/340
axial plane: 50/234
NE limb: 79/048

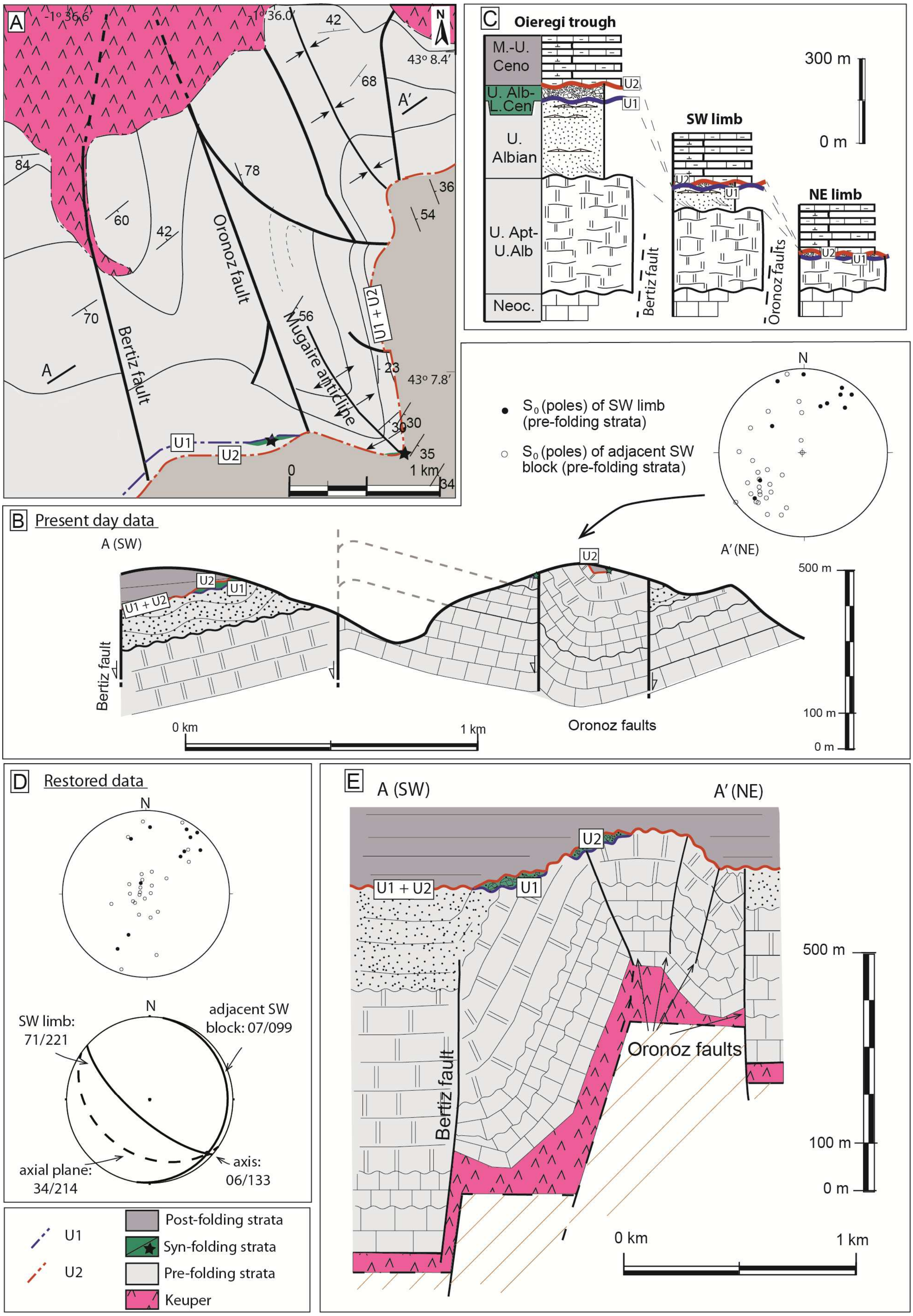
A
Oronoz fault
Bertiz fault
Mugaire anticline
U1
U2
U1 + U2
A
A′
0
1 km
C
Oieregi trough
M.-U. Ceno
U. Alb-L.Cen
U. Albian
U. Apt-U.Alb
Neoc.
SW limb
NE limb
300 m
0 m
Bertiz fault
Oronoz faults
S0 (poles) of SW limb (pre-folding strata)
S0 (poles) of adjacent SW block (pre-folding strata)
N
B
Present day data
A (SW)
A′ (NE)
Bertiz fault
Oronoz faults
0 km
1 km
500 m
100 m
0 m
D
Restored data
N
SW limb: 71/221
adjacent SW block: 07/099
axial plane: 34/214
axis: 06/133
E
A (SW)
A′ (NE)
U1 + U2
Oronoz faults
Bertiz fault
0 km
1 km
U1
U2
Post-folding strata
Syn-folding strata
Pre-folding strata
Keuper

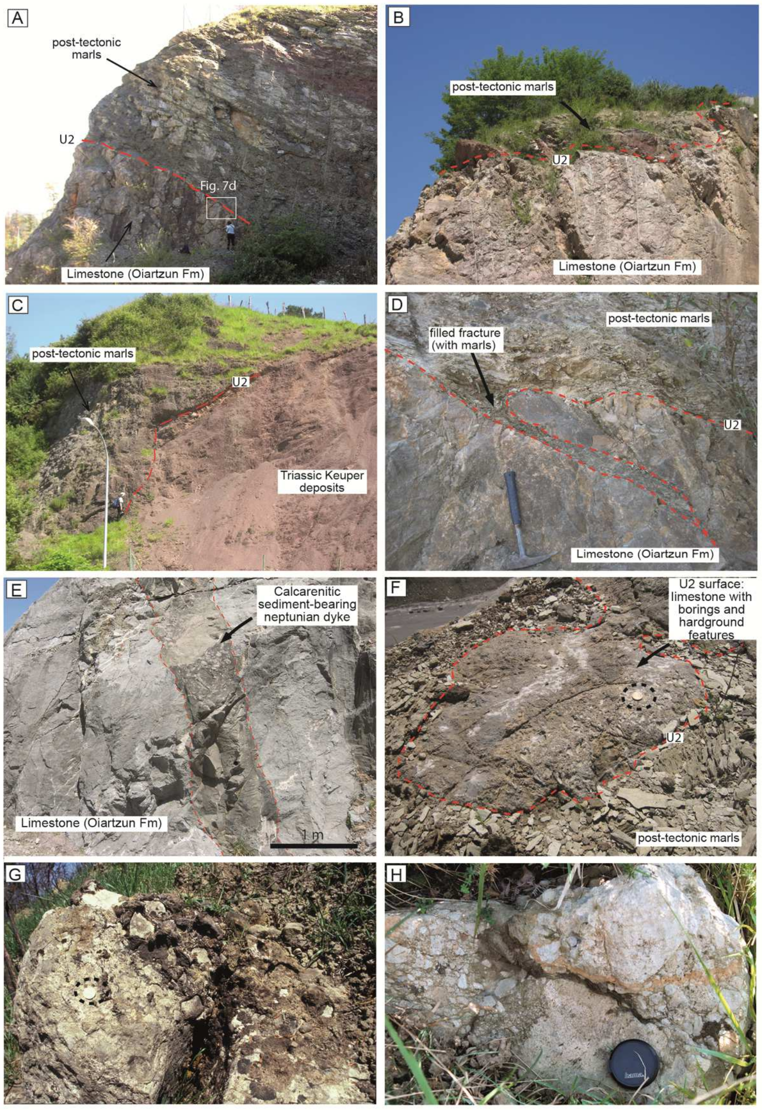
A
post-tectonic marls
U2
Fig. 7d
Limestone (Oiartzun Fm)
B
post-tectonic marls
U2
Limestone (Oiartzun Fm)
C
post-tectonic marls
U2
Triassic Keuper deposits
D
filled fracture (with marls)
post-tectonic marls
U2
Limestone (Oiartzun Fm)
E
Calcarenitic sediment-bearing neptunian dyke
Limestone (Oiartzun Fm)
1 m
F
U2 surface: limestone with borings and hardground features
U2
post-tectonic marls
G
H

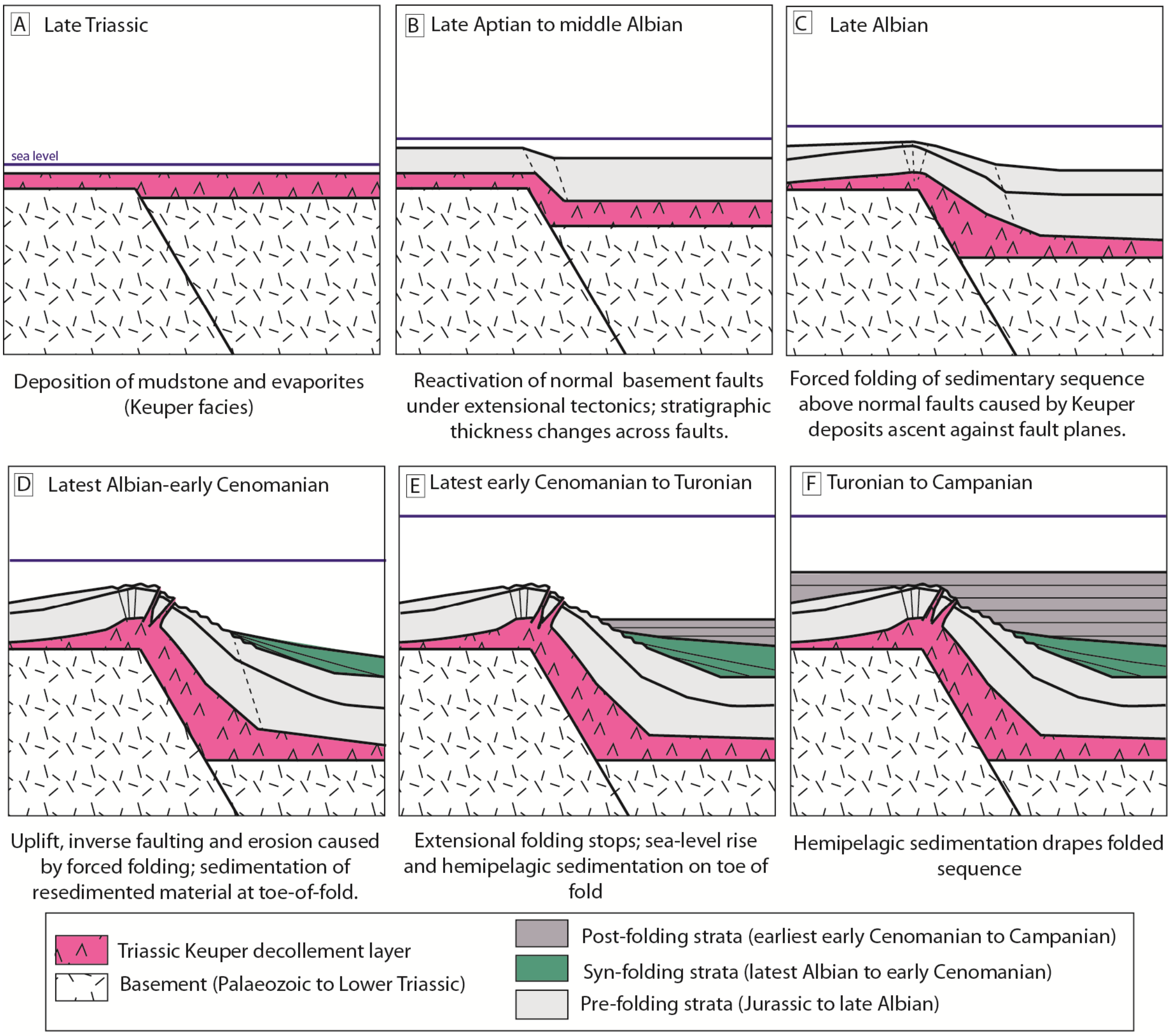
A Late Triassic
sea level
Deposition of mudstone and evaporites (Keuper facies)
B Late Aptian to middle Albian
Reactivation of normal basement faults under extensional tectonics; stratigraphic thickness changes across faults.
C Late Albian
Forced folding of sedimentary sequence above normal faults caused by Keuper deposits ascent against fault planes.
D Latest Albian-early Cenomanian
Uplift, inverse faulting and erosion caused by forced folding; sedimentation of resedimented material at toe-of-fold.
E Latest early Cenomanian to Turonian
Extensional folding stops; sea-level rise and hemipelagic sedimentation on toe of fold
F Turonian to Campanian
Hemipelagic sedimentation drapes folded sequence
Triassic Keuper decollement layer
Basement (Palaeozoic to Lower Triassic)
Post-folding strata (earliest early Cenomanian to Campanian)
Syn-folding strata (latest Albian to early Cenomanian)
Pre-folding strata (Jurassic to late Albian)

Structural, stratigraphic and sedimentological data evidence the growth of forced-folds in a rift margin.

Stratigraphic data suggest that folding occurred during late Albian to early Cenomanian.

The presence of a ductile layer triggered halokinesis related to basement faults in an extensional setting.